Available online at www.sciencedirect.com
SCIENCE DIRECT
Precambrian Research 144 (2006) 213–238
Precambrian Research
www.elsevier.com/locate/precamres

New Precambrian palaeomagnetic constraints on the position of the North China Block in Rodinia

Shihong Zhang [a], Zheng-Xiang Li [b,*], Huaichun Wu [a]

[a] *State Key Laboratory of Geological Processes and Mineral Resources, School of Earth Sciences and Resources, China University of Geosciences, Beijing 100083, China*
[b] *Tectonics Special Research Centre, School of Earth and Geographical Sciences, The University of Western Australia, Crawley (Perth) WA 6009, Australia*

Received 16 November 2004; received in revised form 10 October 2005; accepted 4 November 2005

Abstract

We report new palaeomagnetic results from a ca. 1300 to 800 Ma continental shelf succession on the southern margin of the North China Block. A total of 386 oriented core samples were subjected to stepwise demagnetisation. Two overprint components ('A' and 'B') were identified, with 'A' being a Recent geomagnetic field component and 'B' a likely Mesozoic remagnetisation related to collision of the North and South China Blocks. An interpreted primary remanence was isolated from six rock units. The most reliable results are as follow, in the order of stratigraphic ascendance. (1) Purple mudstone, muddy sandstone and andesite of the lower Yunmenshan Formation (Rb–Sr age ca. 1270 Ma) yields a high-temperature component that passes both reversal and fold tests and gives a palaeopole at (60.6°S, 87.0°E, A_{95} = 3.7°). (2) Mudstone in the overlying Baicaoping Formation yields a high-temperature component with a palaeopole at (43.0°S, 143.8°E, A_{95} = 11.1°). (3) Purple sandstone of the earliest Neoproterozoic Cuizhuang and Sanjiaotang Formations exhibits a high-temperature component that provides a palaeopole at (41.0°S, 44.8°E, A_{95} = 11.3°). Based on both our new results and a critical selection of available palaeomagnetic data, we construct a preliminary apparent polar wander path (APWP) for the North China Block between 1300 and 510 Ma. Regardless of alternative polarity options applicable to these poles, North China was located within equatorial latitudes for much of this interval. Comparing the North China poles with coeval poles from Laurentia suggests that the two continents were situated on the same plate between 1200 and 700 Ma. North China was thus likely part of the supercontinent Rodinia. Separation of North China and Laurentia occurred between 650 and 615 Ma.

Keywords: Palaeomagnetism; Proterozoic; Palaeogeography; North China; Laurentia; Rodinia

1. Introduction

The North China Block (NCB), also known as the Sino-Korean Craton, has an Archean to Paleoproterozoic basement, and well-developed Mesoproterozoic to Neoproterozoic sedimentary cover successions (e.g. Wang and Qiao, 1984). Palaeogeographic positions of the NCB in the Precambrian, particularly its possible connections with other continents, have long been debated. Researchers traditionally favoured a NCB-Siberia connection during the Archaean and Paleoproterozoic time, and suggested that they may have broken apart during the Mesoproterozoic (e.g. Li et al., 1982, and references therein; Wang et al., 1991; Tang, 1992). Li et al. (1996), based on tectonostratigraphic correlations, suggested that the NCB, Siberia, and Laurentia may have been together from ca. 1.8 Ga until the latest Precam-

* Corresponding author. Tel.: +61 8 6488 2652; fax: +61 8 6488 1037.
E-mail addresses: zli@tsrc.uwa.edu.au (Z.-X. Li), shzhang@cugb.edu.cn (S. Zhang), .

0301-9268/$ – see front matter © 2005 Elsevier B.V. All rights reserved.
doi:10.1016/j.precamres.2005.11.007

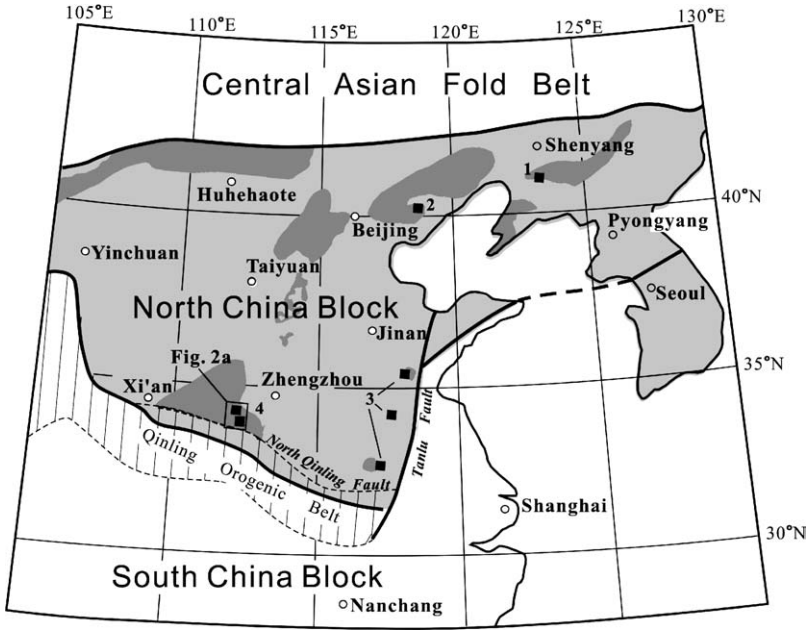

Fig. 1. Locations of Precambrian paleomagnetic investigations in the North China Block (squares). Dark shade shows the distribution of Proterozoic strata. Sample locations: (1) Fuzhou; (2) Jixian; (3) Xu-Huai and (4) Lushan-Ruyang.

brian, and they placed the present north margin of NCB against the western margin of Yenisei Ridge of Siberia. Wang et al. (1997) suggested that the NCB was adjacent to northwestern America during the Meso- to Neoproterozoic, mainly from biogeographical analyses. Based on similarities between Archaean to Paleoproterozoic magmatic and sedimentary rocks, Zhao et al. (2002, 2003) proposed that the East Block of the NCB and the South Indian Block were together as part of a ca. 1.8 Ga supercontinent, and subsequently separated by ca. 1.4 Ga.

Palaeomagnetism is the most discriminating tool for distinguishing between these competing models. However, efforts have been hampered by the sparsity of high quality results from North China and Siberia. Several palaeomagnetic investigations have been carried out in the Meso- to Neoproterozoic successions of the NCB (numbered in Fig. 1): 1. late Precambrian succession in the Fuzhou region, eastern Liaoning Province (Gao and Fan, 1983; Lin, 1984); 2. Paleo- to Mesoproterozoic type section in the Jixian region (Zhang and Li, 1980; Zhang and Zhang, 1985; Lin, 1988; Chumakov and Elston, 1989; Zhang et al., 1991); 3. late Precambrian–Cambrian successions in the region from southern Shandong to northern Anhui Provinces (generally called the Xu-Huai region; Fang et al., 1983; Piper and Zhang, 1997); and 4. the Neoproterozoic–Cambrian succession in the Lushan region, western Henan Province (Zhang et al., 2000). In addition, there is a precisely dated pole from ca. 1.77 Ga dykes in the Datong-Fuping region (Halls et al., 2000). However, severe conflicts exist between some of these results. Possible reasons include: (1) inefficient removal of magnetic overprints, (2) insufficient numbers of samples, and (3) lack of modern demagnetisation and data analysis techniques.

In this paper, we report new palaeomagnetic results from a systematic investigation of late Mesoproterozoic successions in western Henan Province, close to the southern margin of the NCB. Based on these results and a critical selection of existing data, we discuss palaeogeographic positions of the NCB in the period from ca. 1300 to ca. 530 Ma and its possible connection to Rodinia.

2. Geological framework

2.1. Structural and tectonic background

The metamorphic basement of the NCB was consolidated during the ca. 1850 Ma Luliangian orogenic event that united the West and East Archaean Blocks (e.g. Zhao et al., 2002). Soon after 1800 Ma, aulacogens were developed in the NCB; one at the southern margin, east of Xi'an (Fig. 1), containing the volcanic and siliciclastic rocks of the Xiong'er and Ruyang Groups (Wang, 1986) (see Section 2.2).

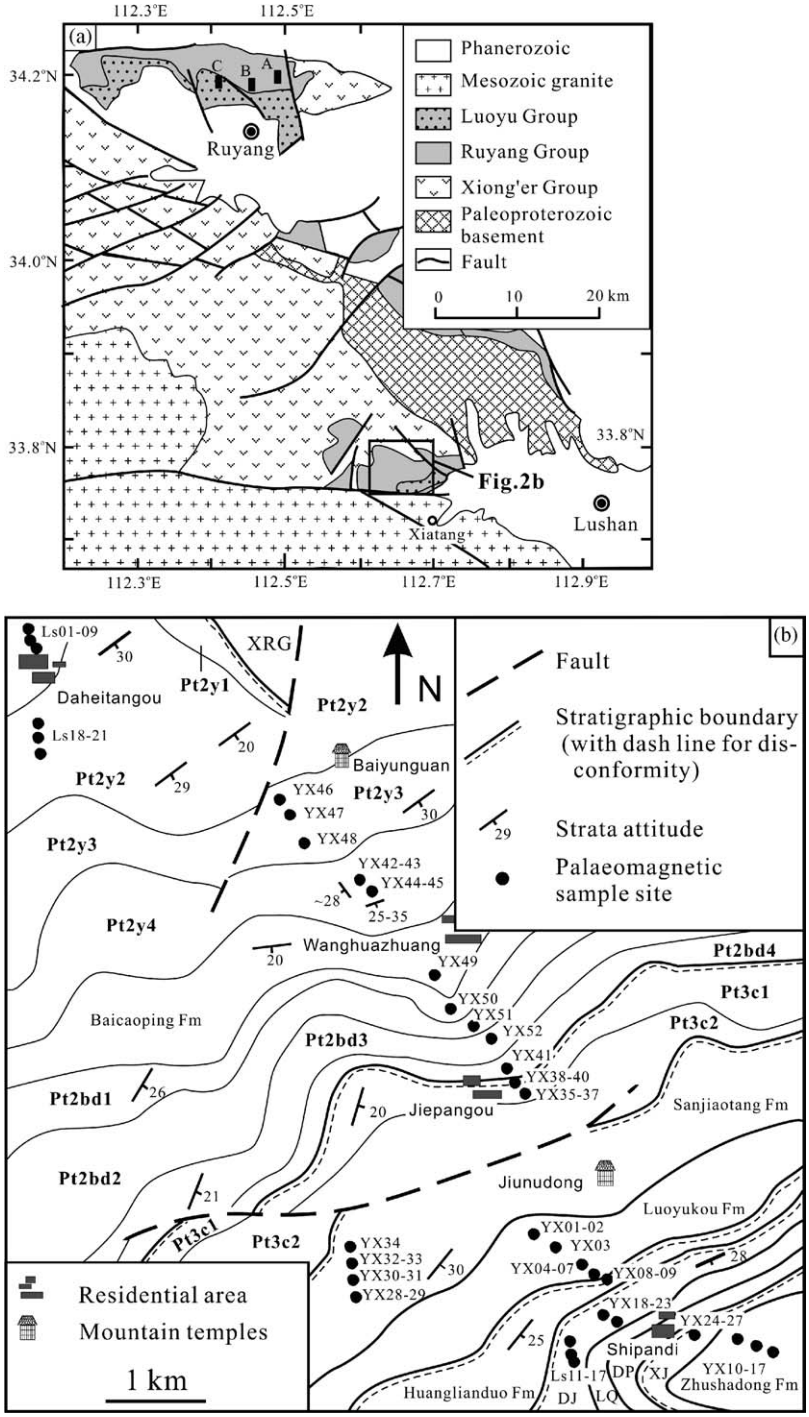

Fig. 2. Simplified geological map of the Ruyang-Lushan region (a) and a more detailed map of the sampled succession in the Lushan region (b). (A)–(C) in (a) are locations of sampled successions in the Ruyang region, with detailed stratigraphic locations of the samples shown in Fig. 3. Abbreviations in (b): XRG—Xionger Group; Pt2y1, Pt2y2, Pt2y3, Pt2y4—Memebers 1–4 of the Yunmengshan Formation; Pt2bd1, Pt2bd2, Pt2bd3, Pt2bd4—Members 1–4 of the Beidajian Formation; Pt3c1, Pt3c2—Members 1–2 of the Cuizhuang Formation; DJ—Dongjia Formation; LQ—Luoquan Formation; DP—Dongpo Formation; XJ—Xinji Formation.

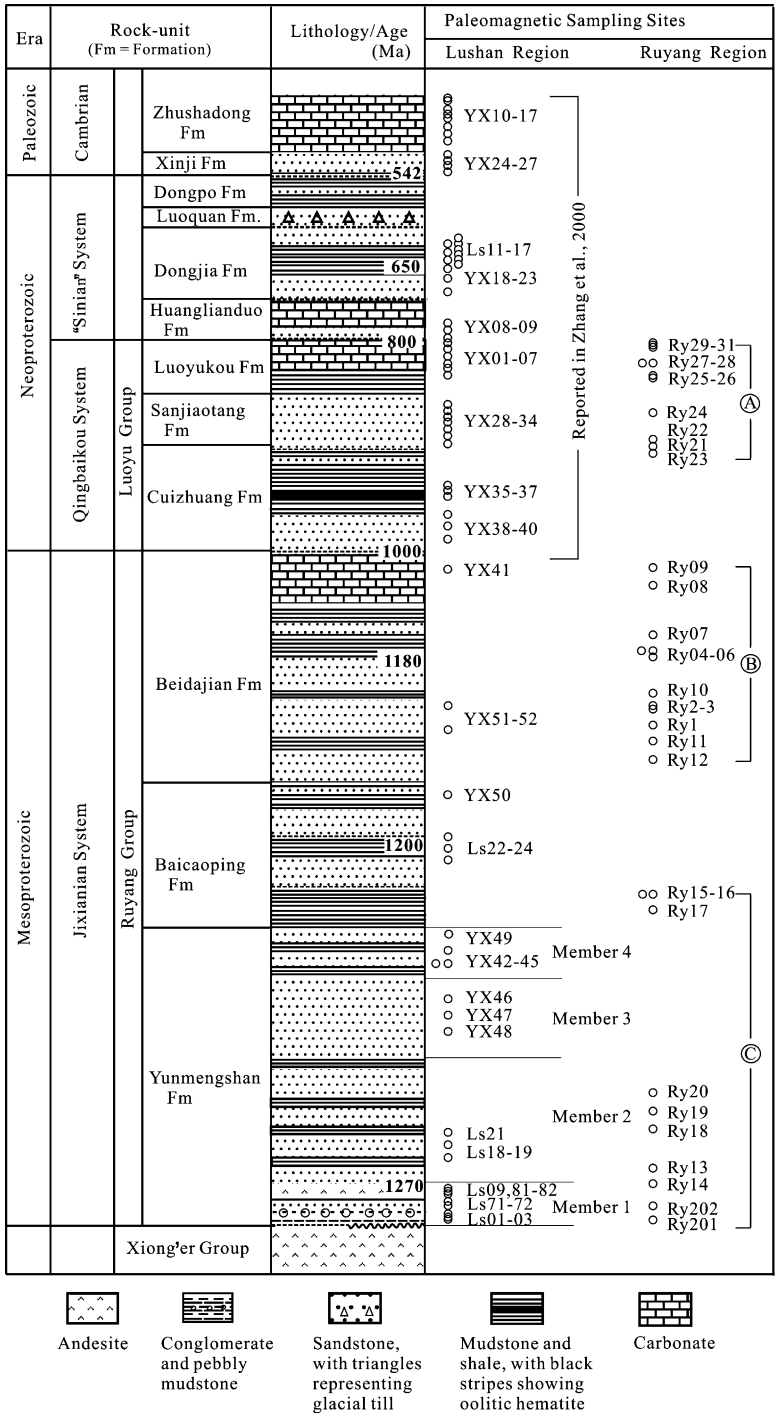

Fig. 3. A composite stratigraphic column with paleomagnetic sampling sites in the Ruyang and Lushan regions. (A), (B) and (C) in circles show the sampled sections in the Ruyang region, as in Fig. 2a.

The southern margin of the NCB is now bounded by the Qinling orogenic belt. Three major orogenic events at ca. 1000 Ma, 430–340 Ma, and 260–155 Ma (Li et al., 1989; Reischmann et al., 1990; Zhang et al., 1994; Li, 1998) have been reported in the orogen. The first is interpreted to represent a terminal Mesoproterozoic convergent margin along the southern margin of the NCB (Li et al., 1996, and references therein). This event is iden-

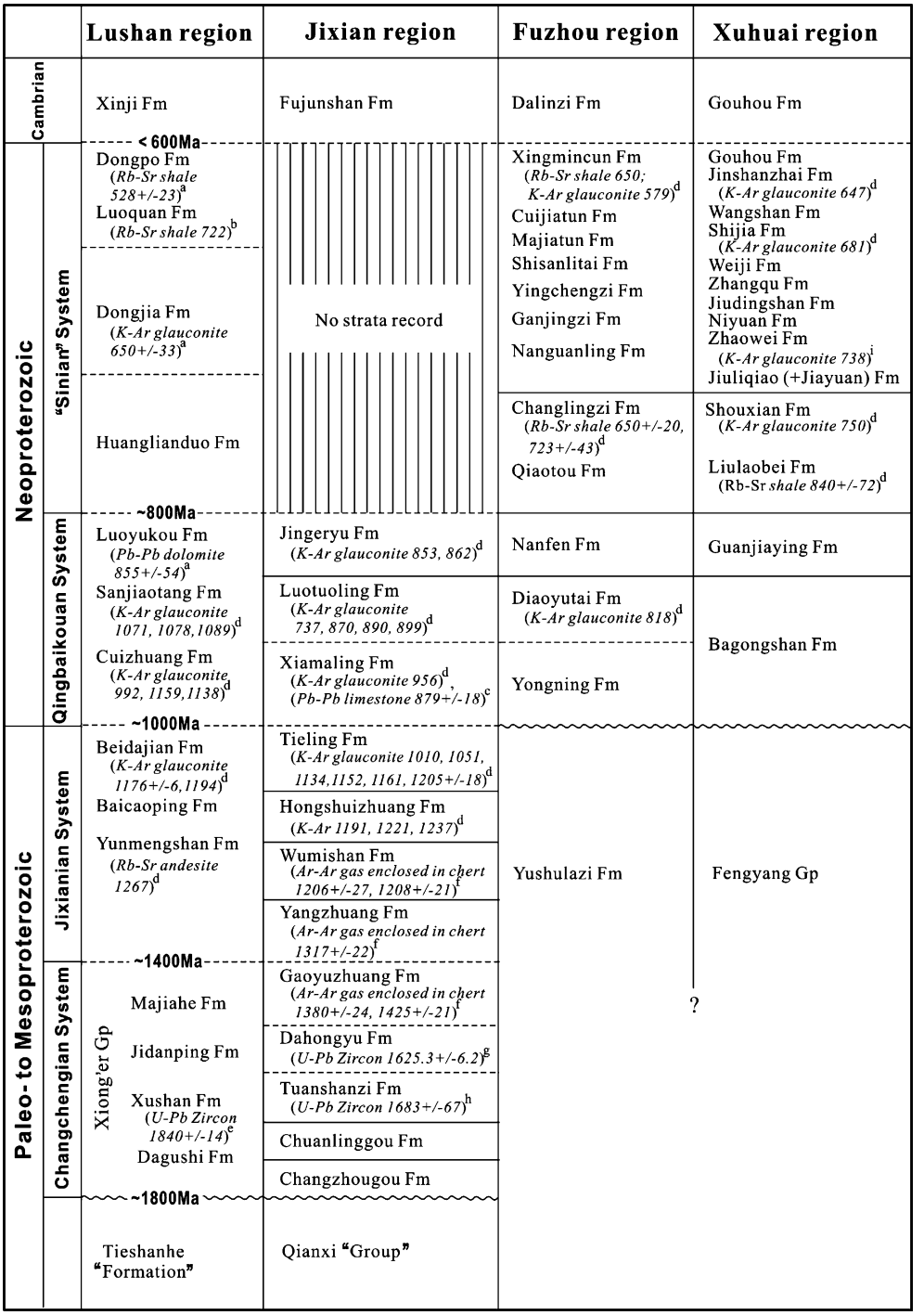

Fig. 4. Stratigraphic correlation of Meso-Neoproterozoic rocks in the NCB. Modified from Xing (1989, Table 9 and Table 21) and Qiao et al. (2001), (Tables 1–1, 1–4). Fm: Formation; Gp: Group. Italics in brackets show isotopic age information (method, rock or mineral, age in Ma). Sources of data: (a) Guan et al. (1983); (b) Li et al. (1985); (c) Qiao and Gao (1997); (d) Xing (1989); (e) Sun et al. (1991); (f) Wang et al. (1995); (g) Lu and Li (1991); (h) Li et al. (1995); (i) Fang et al. (1983).

tified by a disconformity between the Mesoproterozoic and Neoproterozoic strata in the study region (Wang and Qiao, 1984; Zhou et al., 1996). The second event, mainly restricted to central Qinling belt, was accompanied by ~430–340 Ma magmatism, and is interpreted as due to a possible arc-continent collision (Zhang et al., 1994; Meng and Zhang, 1999, 2000), but no related deformation has been reported on the NCB proper (including the study region). The last event is widely regarded to correspond to collision between the NCB and South China Block (SCB) between ca. 260 and 155 Ma (Li, 1998 and references therein), as first suggested by palaeomagnetic results (Zhao and Coe, 1987; Zhao et al., 1996; Enkin et al., 1992). This event is the only one that affected the study region, producing monoclinal dips of 15°–35° toward the southeast (Fig. 2). At outcrop scale, minor folds are seen in some of the Precambrian formations. There is no evidence to indicate any vertical-axis rotation between the study region and the rest of the NCB.

2.2. Stratigraphy and age constraints

Our study areas are in west Henan Province, close to the southern margin of the NCB. The strata there range from upper Mesoproterozoic to Lower Cambrian, and the structures are simple (Figs. 1 and 2). We show in Fig. 3 a simplified stratigraphy of the study region, and in Fig. 4 stratigraphic correlations (with some absolute age constraints) with other successions in the NCB.

The chronological framework for the Precambrian strata in the NCB is largely established through biostratigraphy and regional correlations (e.g. Wang, 1986; BGHNP, 1989; Xing, 1989), and reliable isotopic ages are rare. Most results were obtained using the glauconite K–Ar and Rb–Sr whole-rock methods on shale and volcanic rock. A few ages are from carbonate rocks using the Pb–Pb method. The available age data from both the southern margin of the NCB and its northern part (e.g. the Jixian section) are summarized in Fig. 4. A few ages are apparently out of stratigraphic order, and should therefore be treated with extreme caution. One is the age for the Luoquan glacial diamictite. Although other opinions exist (Li et al., 1985; Liu, 1991), the evidence suggests a latest Precambrian age for this glacial unit (Guan et al., 1980, 1983; Xing, 1989; Yin and Guan, 1999).

3. Sampling and measurements

We collected palaeomagnetic samples from two regions: the Lushan region in the south and the Ruyang region about 50 km to the north (Fig. 2a). A total of 386 core samples were collected using gasoline-powered drills. Samples were oriented using a magnetic compass and a sun compass when possible. Sampling in the Lushan region was carried out along a ~5 km long section (Fig. 2b) known as the Daheitangou-Wanghuazhuang section (BGHNP, 1989). In the Ruyang region, the Yunmengshan, Baicaoping and Beidajian formations were sampled along roadsides, and Neoproterozoic strata sampled along the western bank of the Shanghongjian reservoir (A, B and C in Fig. 2a). Each sampling site normally covers 5–20 m of stratigraphic section with samples cored following stratigraphic order. The sampled rocks include purple fine-clastic sandstone, muddy sandstone, siltstone, and muddy dolomite.

Each core sample was cut into multiple 22 mm-long specimens. Demagnetisation and magnetic measurements were carried out in the Palaeomagnetism Laboratory of The University of Western Australia (UWA) and that of the Institute of Geology and Geophysics at the Chinese Academy of Sciences (CAS). Remanence measurements in both laboratories were carried out using 2G-Enterprise three-axis cryogenic magnetometers housed in room-size Helmholtz coils, with a low magnetic field (~100 nT) in the sample-loading region. AF demagnetisation was carried out using a 2G-600 automated AF demagnetizer attached to the cryogenic magnetometer, and thermal demagnetisation using MMTD18 (at UWA) and MMTD60 (at CAS) furnaces, also housed inside the Helmholtz coils. During the experiments, samples were further protected from magnetic contamination by μ-metal shielding. All samples were subjected to stepwise demagnetisation. Thermal treatments were applied to all reddish specimens, with temperature steps ranging from 50–150 °C at low-temperatures to 5–20 °C at temperatures above 570 °C. Some samples were treated by low-temperature (<300 °C) thermal demagnetisation first to eliminate any remanence carried by goethite, followed by alternating field (AF) demagnetisation to isolate remanence carried by magnetite.

4. Palaeomagnetic results

To determine the magnetic remnant components, both the ROCKMAG software package developed at the Rock Magnetism Laboratory of the Commonwealth Science and Industry Research Organization, Australia, and R. Enkin's palaeomagnetic software, were used. Identification of magnetic components was carried out mainly by the line fitting method (Kirschvink, 1980), but sometimes by using stable end-points. In general, remanence components fall into three categories: (1) a Recent field overprint (component 'A') normally as a low- to medium-temperature component; (2) a Mesozoic overprint (com-

Table 1
Interpreted overprints of Recent/Mesozoic geomagnetic field (components A and B), Lushan-Ruyang region, western Henan Province

Rock-unit, sampled location	Comp.	n_o	n	nr	Coord.	Direction			α_{95}	Palaeopole			
						D	I	k		Plat	Plon	dp	dm
Member 1, Yunmengshan Fm, Lushan	A	51	48	0	G	3.8	45.0	19.7	4.8	82.1	267.3	3.8	6.1
					S	22.8	59.7	19.3	4.8	70.7	175.6	5.4	7.2
Member 2, Yunmengshan Fm, Lushan	A	32	27	0	G	2.4	48.1	14.3	7.6	84.9	268.3	6.5	9.9
					S	30.6	62.2	13.7	7.8	64.4	171.4	9.4	12.1
Lower, Yunmengshan Fm, Ruyang	A	37	26	0	G	5.3	47.8	11.4	8.8	83.0	251.1	7.5	11.5
					S	355.8	56.4	10.3	9.3	85.6	62.2	9.7	13.4
Volcanic bed, Yunmengshan Fm, Ruyang	A	20	20	0	G	5.9	52.1	84.5	3.6	84.8	218.2	3.4	4.9
					S	6.0	47.1	84.8	3.6	82.1	250.2	3.0	4.7
Member 3, Yunmengshan Fm, Lushan	A	21	19	0	G	357.0	52.0	11.9	10.2	87.2	358.3	9.5	14.0
					S	32.4	64.5	10.8	10.7	62.5	165.8	13.8	17.2
Member 4, Yunmengshan Fm, Lushan	A–HT	25	13	3	G	2.5	36.8	11.1	13.0	76.5	282.6	8.9	15.2
					S	1.6	59.7	11.9	12.6	83.1	122.9	14.3	19.0
	A–LT	25	22	0	G	9.9	44.0	14.7	8.4	78.3	243.1	6.6	10.5
					S	21.3	65.6	8.6	11.2	68.8	155.1	14.8	18.2
Top Yunmenshan Fm, Lushan	B(1)	9	8	1	G	334.9	12.9	32.1	9.9	54.2	338.7	5.1	10.1
					S	337.8	35.6	33.5	9.7	65.8	352.7	6.5	11.2
Lower Baicaoping Fm, Lushan	A	19	19	0	G	14.8	45.1	15.9	8.7	75.4	228.0	7.0	11.0
					S	44.4	53.0	16.2	8.6	53.3	190.2	8.2	11.9
Baicaoping Fm, Ruyang	A	29	17	0	G	13.9	53.5	8.4	13.1	78.5	199.6	12.7	18.2
					S	22.5	75.4	8.4	13.1	58.4	132.2	22.0	24.0
Beidajian, top Baicaoping Fm, Lushan	A	26	24	1	G	6.6	47.2	8.5	10.5	82.2	244.8	8.9	13.7
					S	32.5	59.2	8.5	10.5	63.4	179.7	11.8	15.9
	B(2)	26	18	1	G	351.7	9.9	23.0	7.4	60.2	309.5	3.8	7.5
					S	355.9	28.7	23.1	7.3	71.1	305.0	4.4	8.0
Beidajian Fm, Ruyang	A	70	62	0	G	355.9	41.4	8.4	6.6	78.9	312.4	4.9	8.1
					S	347.5	62.3	8.1	6.8	76.5	70.2	8.3	10.6
	B(3)	70	65	0	G	7.3	16.1	19.0	4.1	63.1	276.4	2.2	4.2
					S	7.1	37.5	18.2	4.2	75.3	265.4	2.9	4.9
Luoyu Fm, Ruyang	A	26	15	0	G	354.5	55.8	54.7	5.2	85.0	49.1	5.3	7.5
					S	356.5	74.0	44.3	5.8	64.0	108.5	9.4	10.5
	B	26	25	0	G	331.6	52.5	34.0	5.0	66.4	27.7	4.7	6.9
					S	317.0	68.6	35.0	5.0	54.7	65.8	7.1	8.5

For rock unit see Figs. 3 and 4; Sample locations: Lushan (33.80°N, 112.65°E), Ruyang (34.25°N, 112.50°E); Fm, Formation; Comp., components defined, where numbers in brackets following B are for use in Fig. 10; n_o, number of samples demagnetized; n, number of samples used for statistical average; nr, number of samples with reversed polarity; Coord., coordinates, where G is the geographic coordinates; S, stratigraphic coordinates; D, declination; I, inclination; k, Fisher precision parameter for direction; α_{95}, radius of circle of 95% confidence about the direction. Plat/Plon, north latitude/east longitude of VGP; dp/dm, semi-axes of elliptical error around the pole at a probability of 95%.

ponent 'B'); and (3) a high-temperature component of likely primary origin. The two overprint components are listed in Table 1, and directions of the interpreted primary component are given in Table 2. We describe below all remanence data from the studied rock units, and give a summary discussion on the origin of the components (particularly the primary component) in Section 4.6. Representative demagnetisation plots are given in Fig. 5, and stereographic plots in Figs. 6–8.

4.1. Lower Yunmenshan Formation

The Yunmengshan Formation is 1022 m thick along the sampling section in the Lushan region. It is subdivided into four members in an ascending order (Fig. 3). The lower part of the Yunmengshan Formation in both the Lushan and Ruyang regions was formed in fluvial environments. The strata disconformably overlie volcanic rocks of the Xiong'er Group. Stable magnetic

Table 2
Interpreted primary remanence for Meso- to Neoproterozoic successions in western Henan Province

Site	n/nr (n_o)	Coor.	Direction			α_{95}	Palaeopole			
			D	I	k		Plat	Plon.	dp	dm
(1) Lower part of the Yunmengshan Formation										
Member 1, Yunmengshan Fm, in the Lushan region (33.8N;112.65E)										
Ls01	8 (8)	G	12.4	−4.1	20.3	12.6	52.3	272.1	6.3	12.6
		S	12.9	8.7	20.3	12.6	58.2	267.6	6.4	12.7
Ls03	9 (9)	G	19.5	−7.6	12.1	15.4	48.1	262.7	7.8	15.5
		S	19.2	7.2	12.5	15.1	54.9	257.8	7.6	15.2
Ls71	6 (6)	G	8.7	−4.8	29.5	12.6	52.9	278.1	6.3	12.6
		S	10.0	13.9	29.5	12.5	61.7	271.3	6.5	12.8
Ls72	6 (6)	G	10.6	−5.0	82.7	7.4	52.3	275.1	3.7	7.4
		S	11.9	13.0	82.2	7.4	60.6	268.0	3.8	7.5
Ls81	7 (7)	G	17.6	−3.6	30.3	11.2	50.7	264.1	5.6	11.2
		S	18.4	9.9	30.2	11.2	56.5	257.9	5.7	11.3
Ls82	6 (6)	G	5.0	6.4	25.6	13.5	59.1	282.9	6.8	13.6
		S	7.6	21.0	25.5	13.5	66.0	274.0	7.5	14.2
Ls09	8 (9)	G	11.3	−2.0	13.1	15.9	53.6	273.4	8.0	15.9
		S	12.1	10.6	12.2	16.5	59.4	268.4	8.5	16.7
Member 2, Yunmengshan Formation, in the Lushan region (33.8N; 112.65E)										
Ls18	9/5 (10)	G	199.8	−1.3	6.5	21.9	−52.0	79.3	11.0	21.9
		S	203.6	−15.3	7.0	20.9	−56.1	67.3	11.0	21.5
Ls21	6/3 (8)	G	201.4	14.5	13.2	19.2	−44.1	82.4	10.1	19.7
		S	198.6	1.8	12.7	19.5	−51.1	82.1	9.8	19.5
Lower part of Yunmengshan Formation, in the Ruyang region (34.25N; 112.5E)										
Ry13	8/3 (13)	G	180.3	−9.0	6.2	24.2	−60.3	111.9	12.3	24.4
		S	178.9	−7.5	6.4	23.8	−59.5	114.7	12.1	24.0
Ry18	9 (9)	G	18.3	6.1	7.2	20.6	54.5	259.9	10.4	20.7
		S	19.1	24.0	7.3	20.5	62.2	249.2	11.7	21.9
Ry19	7 (7)	G	7.1	5.9	18.2	14.5	58.0	279.0	7.3	14.6
		S	6.6	24.9	19.2	14.1	68.0	275.1	8.1	15.1
Ry20	6/2 (8)	G	185.0	13.4	6.8	27.8	−48.7	105.0	14.5	28.4
		S	185.0	−5.0	6.3	29.0	−57.9	103.1	14.6	29.1
Ry201	6 (9)	G	5.0	28.5	30.5	12.3	70.4	278.0	7.4	13.5
		S	5.1	23.5	30.7	12.3	67.5	279.4	7.0	13.1
Ry202	7 (11)	G	16.4	22.1	110.6	5.8	62.8	255.3	3.2	6.1
		S	16.1	17.2	110.7	5.8	60.6	258.6	3.1	6.0
Mean pole for the lower Yunmengshan Formation, averaging on site level										
"Normal"*	$N1 = 4$	G					−52.1	93.5	$A_{95} = 13.7$	
		S					−57.5	90.8	$A_{95} = 13.8$	
"Reversed"*	$N2 = 11$	G					56.2	270.7	$A_{95} = 4.5$	
		S					61.7	265.4	$A_{95} = 3.4$	
Mixed Polarities	$N = 15$	G					−55.1	91.5	$A_{95} = 4.3$	
		S					−60.6	87.0	$A_{95} = 3.7$	
(2) Member 3, Yunmengshan Formation, in the Lushan region, averaging on sample level										
	9/4 (21)	G	111.5	25.9	6	22.9	−9.5	179.1	13.4	24.7
		S	113.5	1.3	5.9	23.1	−19.0	188.5	11.6	23.1
(3) Lower part of Member 4, Yunmengshan Formation, in the Lushan region, averaging on sample level										
	10 (25)	G	68.0	50.9	10.1	16.0	33.8	184.6	14.6	21.6
		S	97.7	46.3	15.1	12.8	9.2	175.4	10.5	16.4
(4) Baicaoping Formation										
Ls22-24	7/1 (19)	G	175.5	40.8	11.2	18.8	−32.7	117.6	13.8	22.8
		S	167.0	20.7	12.5	17.8	−43.8	130.5	9.8	18.7

Table 2 (*Continued*)

Site	*n*/nr (n_o)	Coor.	Direction			α_{95}	Palaeopole			
			D	*I*	*k*		Plat	Plon.	dp	dm
Ry15-17	7/1 (29)	G	143.6	23.8	12.3	17.9	−31.9	155.5	10.2	19.1
		S	147.7	8.4	12.2	18.0	−40.9	157.4	9.1	18.1
Mean pole, average on sample level										
	14	G					−32.7	136.0	$A_{95} = 13.8$	
		S					−43.0	143.8	$A_{95} = 11.1$	
(5) Lower part of the Cuizhuang Formation in the Lushan region (after Zhang et al., 2000)										
YX35-40	19 (37)	G	33.3	24.2	52.0	4.7	53.1	229.5	2.7	5.0
		S	43.3	27.8	65.0	4.2	46.6	217.8	2.5	4.6
(6) Upper part of the Cuizhuang Formation in the Ruyang region										
Ry21-23	14/2 (21)	G	223.7	−1.2	6.0	17.8	−37.1	52.5	8.9	17.8
		S	222.2	−6.4	9.9	13.3	−40.0	51.4	6.7	13.4
(7) Sanjiaotang Formation in the Lushan region (after Zhang et al., 2000)										
YX28-34	20/6 (45)	G	222.8	−14.4	10.6	10.5	−42.5	46.6	5.5	10.8
		S	229.0	−8.8	11.6	10.0	−35.9	44.4	5.1	10.1

*The assigned polarities here are arbitrary, thus marked with "". *n*/nr (n_o), total sample number/reversed sample number (total number of samples demagnetized). *N*, site number. A_{95}, radius of circle of 95% confidence about the palaeopole. Other abbreviations are the same as in Table 1.

remanence has been isolated mostly from purple mudstone, muddy sandstone and volcanic rock.

Samples from Member 1 (sites Ls01-03, 71, 72, 81, 82, 09) and Member 2 (sites Ls18-21) in the Lushan region were all from purple mudstone and muddy sandstone. The NRM intensities of the mudstone samples are 1–10 mA m^{-1}, whereas NRM in the sandstone samples are mostly on the order of 1 mA m^{-1}.

Two components have been identified from Member 1 strata in the Lushan region. A lower-temperature component (component 'A') is defined mostly below ca. 650 °C (Fig. 5a, Ls08D). It has a northerly declination and downward inclination before structural correction with an average direction of $D = 3.8°$, $I = 45°$, $n = 48$, $\alpha_{95} = 4.8°$, which resembles that of the local present geomagnetic field ($D = 356.5°$, $I = 50.6°$, after IGRF2000). A high-temperature component of possible primary origin is defined as either linear vectors (Fig. 5a) or stable endpoints between 650 and 680 °C. It has north-easterly shallow directions (Fig. 6a). The high unblocking temperatures indicate that the main magnetic carrier is hematite.

The demagnetisation behaviour of Member 2 samples is similar to that of Member 1, but with lower NRM intensities. After the removal of component 'A' at low temperatures, fifteen samples exhibit a poorly defined but consistent high-temperature component above ca. 650 °C with mixed polarities (Figs. 5b and 6b).

In the Ruyang region, the Yunmengshan Formation is between 191 and 794 m thick. Thirty-eight purple muddy sandstone samples were collected from the lower part of the formation. They have NRM intensities ranging between 1 and 10 mA m^{-1} and demagnetisation behaviour similar to that of Members 1 and 2 of the Yunmengshan Formation in the Lushan region. Two components were isolated from these samples: component 'A' mostly below 600 °C, and a high-temperature component directed either shallowly to the northeast (Figs. 5c and 6c) or to the southwest (Figs. 5d and 6c).

There is one volcanic interlayer in the lower part of Yunmengshan Formation. It is distributed widely in the sampling regions and marks the top of Member 1. Thirteen samples were collected from two sites (RY201–202) from the Ruyang region. The samples yield two components through either AF or thermal demagnetisation (Fig. 5e and f). The soft component 'A' (Table 1) is stable up to ∼20 mT or 500 °C. A hard component is directed shallowly downwards to the northeast, with unblocking temperatures around 575 °C, or coercivities of ∼65 mT, indicating that magnetite is the main remanence carrier.

A ∼15° difference in dip of bedding between the four redbed sites (Ry13, 18, 19, 20) and the two volcanic sites (Ry201, 202) in the Ruyang region enabled a fold test to be conducted. Fisher's precision parameter, *k*, reaches a maximum after about 100% untilting, indicating that the component was acquired before tilting (Fig. 6c). A McFadden (1990) fold test (definition 2) shows that the in situ directions correlate with bedding attitudes at 99% confidence level, but the tilt-corrected directions have no

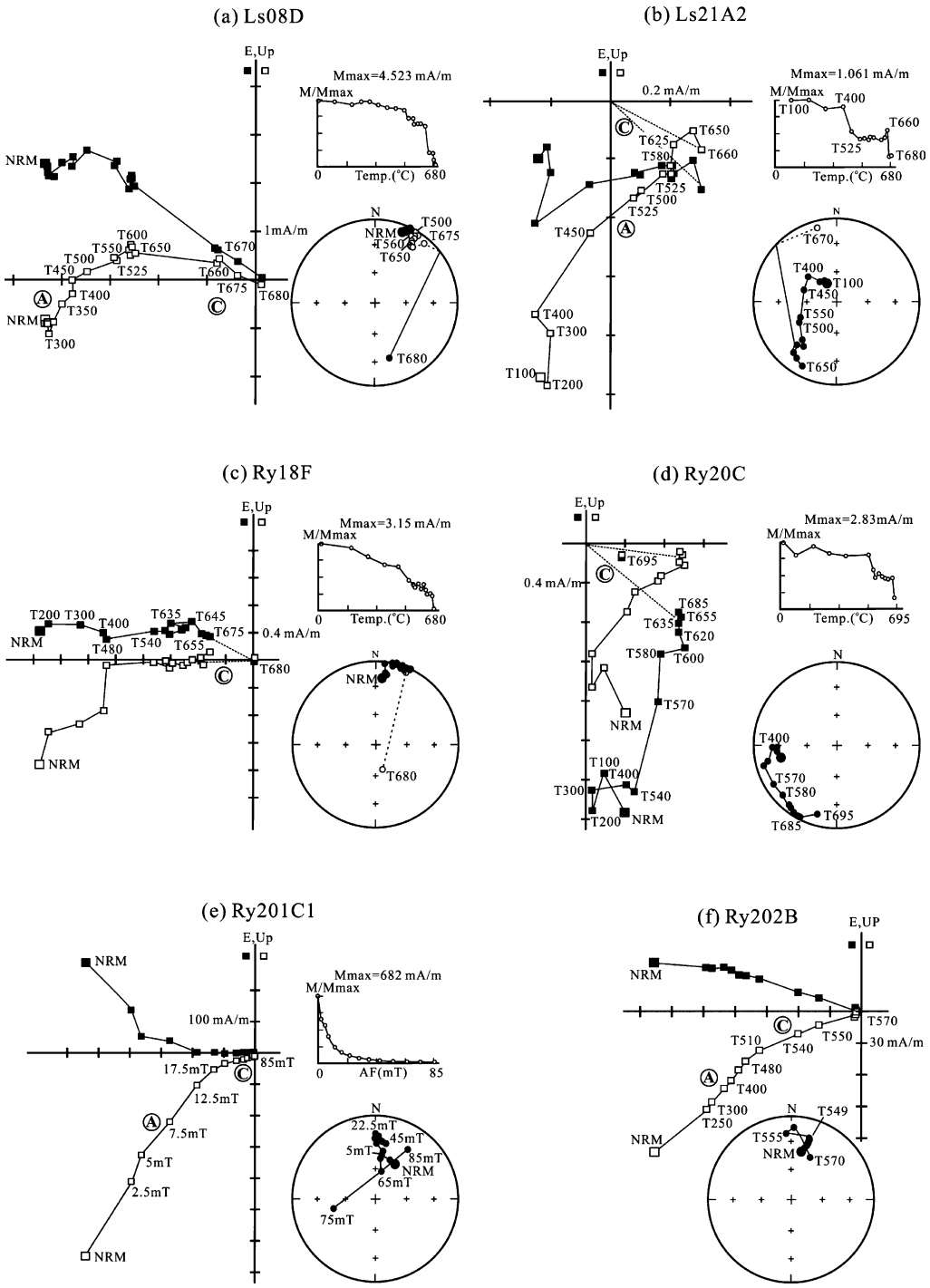

Fig. 5. Results of stepwise demagnetization. In orthogonal vector plots, closed (open) symbols represent projections on the horizontal (vertical) plane. NRM, natural Remanent Magnetization. Plots (e) is of alternating-field demagnetization, and all the rest are of thermal demagnetization, with numbers following 'T' are temperature in °C. (A), (B) and (C) in circles mark the identified remanence components (see details in text). All directions are in situ.

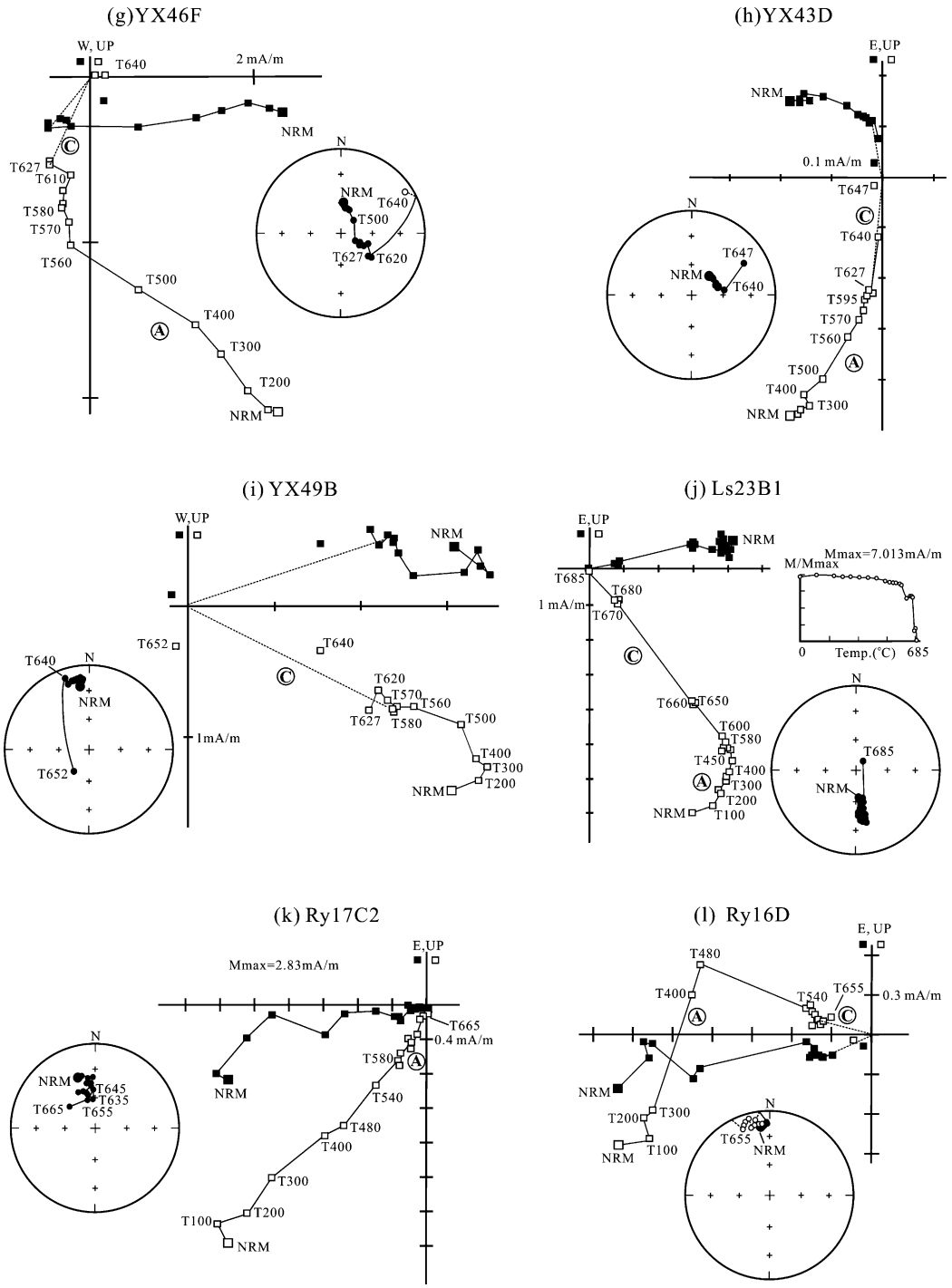

Fig. 5. (*Continued*)

apparent correlation with bedding attitudes, constituting a positive fold test.

At the site-mean level, poles of the characteristic remanence in the lower Yunmengshan Formation of both the Lushan and Ruyang regions pass the McFadden and McElhinny's (1990) reversal test with $\gamma_c = 13.7^\circ$ ('C' class) (Fig. 7). The average palaeomagnetic pole (Fig. 9, pole 1) falls outside the Phanerozoic apparent polar wander path (APWP) of the NCB. This observation, together with the positive fold test and reversal test, suggest that

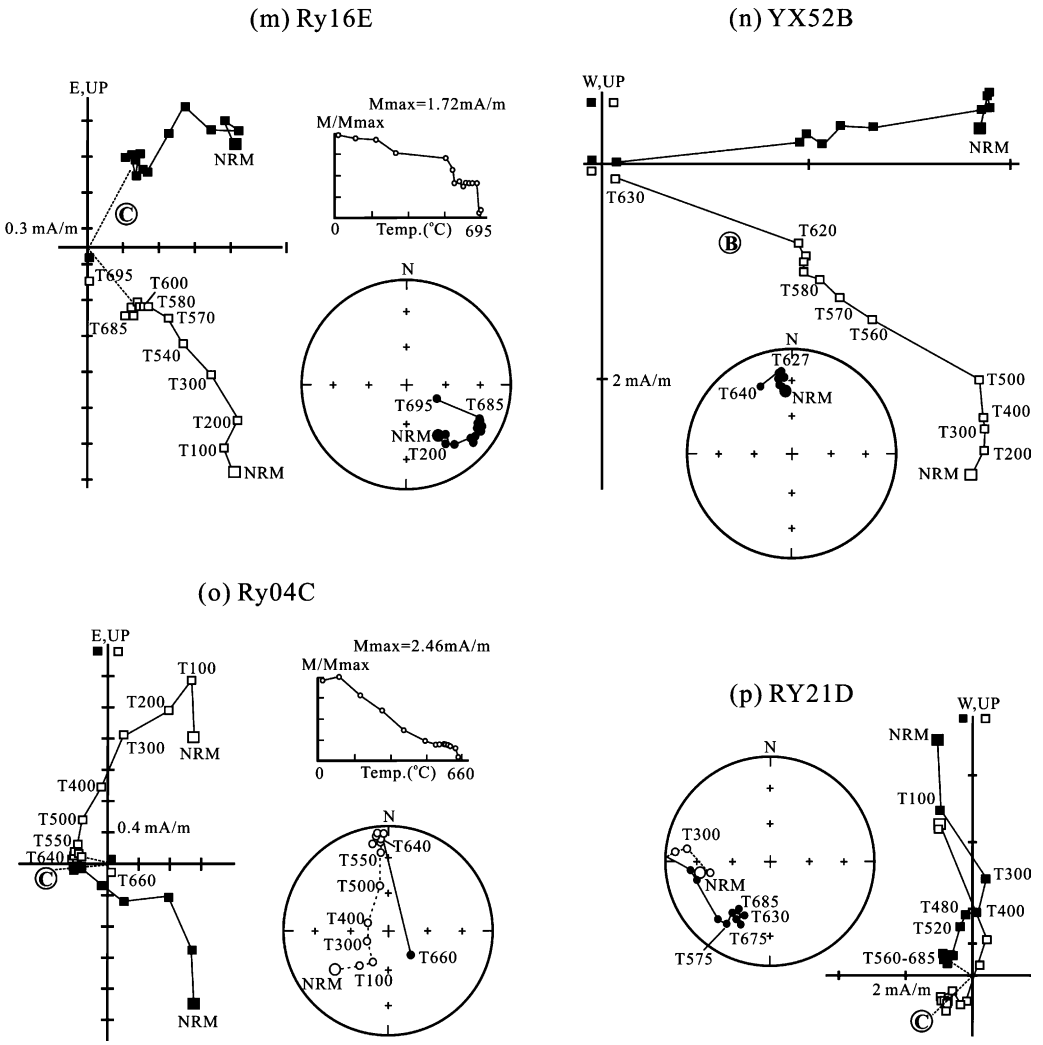

Fig. 5. (*Continued*).

the remanence is likely of primary origin. These palaeomagnetic data are listed in Table 2.

4.2. Upper Yunmengshan Formation

The upper Yunmengshan Formation consists dominantly of purple quartz sandstone. Remanence in these samples is generally weak and unstable during demagnetisation. Samples that showed no linear segments or stable endpoints were excluded from further analysis.

Samples from Member 3 (sites YX46-48) yielded two components. A soft one (component 'A') was stable below 560 °C and its directions are similar to the present geomagnetic field direction (Table 1). A hard component, commonly shown as stable end points in the temperature range of 560–630 °C (Fig. 5g), is directed downward to the east-southeast (Fig. 6d). These directions are clearly different from those in the lower Yunmengshan Formation.

In Member 4 (sites YX42-45 and 49), a small anticline was found in a 20 m-wide outcrop. Twenty-five samples were collected from four sites around this small fold. The demagnetisation behaviour of these samples can be classified into two types. Type 1 samples ($n = 13$) revealed a single component 'A' only, with unblocking temperature around 640 °C. Type two samples yield a high-temperature (570–640 °C) component from ten samples after removing component 'A'. This high-temperature component is directed downwards to between east and south-east (Figs. 5h and 6e). It passes the McFadden (1990) fold test (definition 2): the in situ directions correlate with bedding attitudes at 99% confidence level, but the tilt-corrected directions have

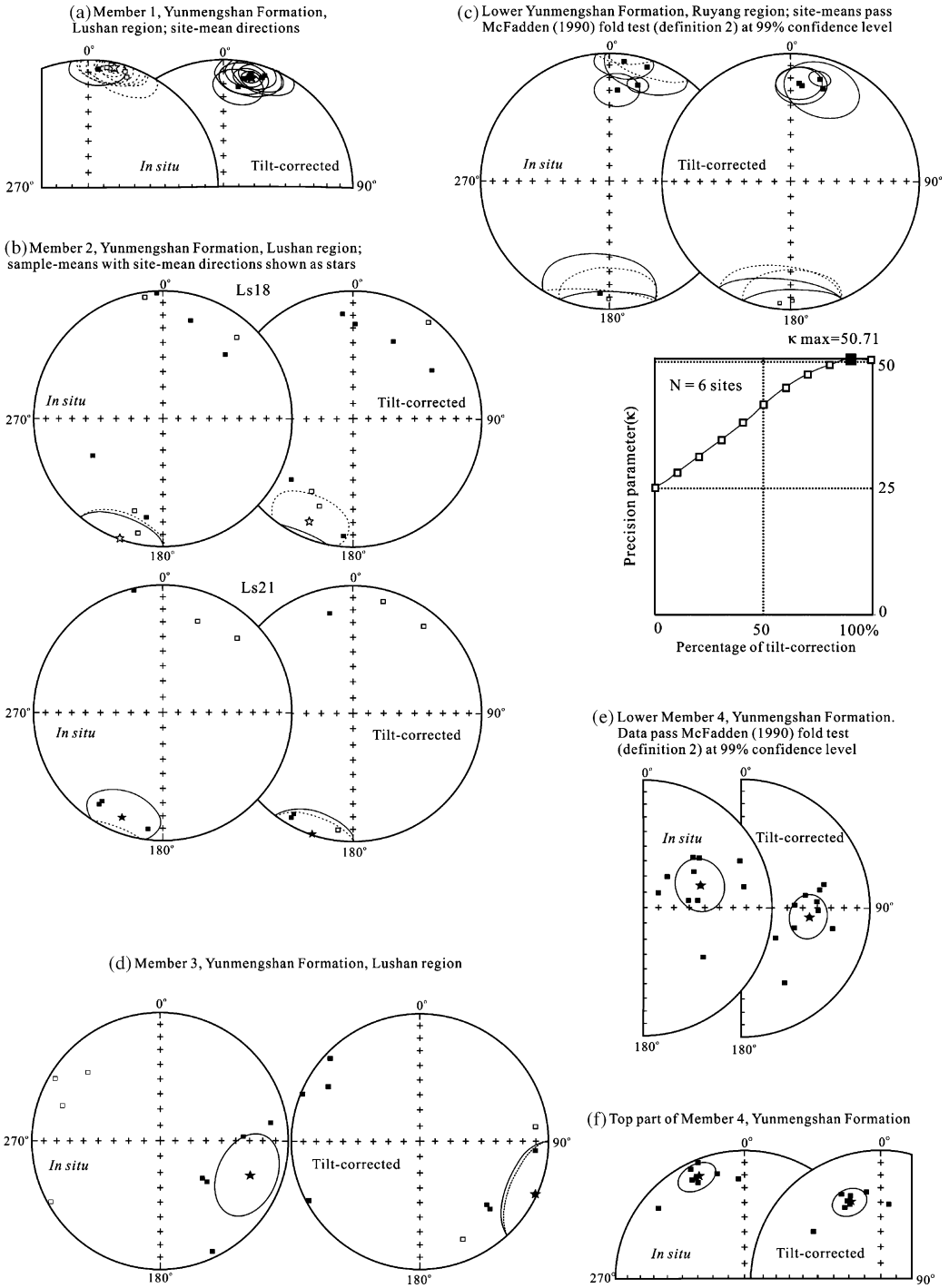

Fig. 6. Stereographic plots of stable remanence directions from the Yunmengshan Formation. Closed (open) symbols represent positive (negative) inclinations, all in equal-area projections. Squares with 95% confidence circles represent site-mean directions, and those without 95% confidence circles are sample-level directions. Stars with 95% confidence circles are mean directions for the rock unites.

no apparent correlation with bedding attitudes. This indicates that the high-temperature component, though retained in less than half of the samples, is of pre-folding origin.

The corresponding palaeopoles from the high-temperature component in Members 3 and 4 of the Yunmengshan Formation are different from the known younger poles for the NCB (poles number 2 and 3 in

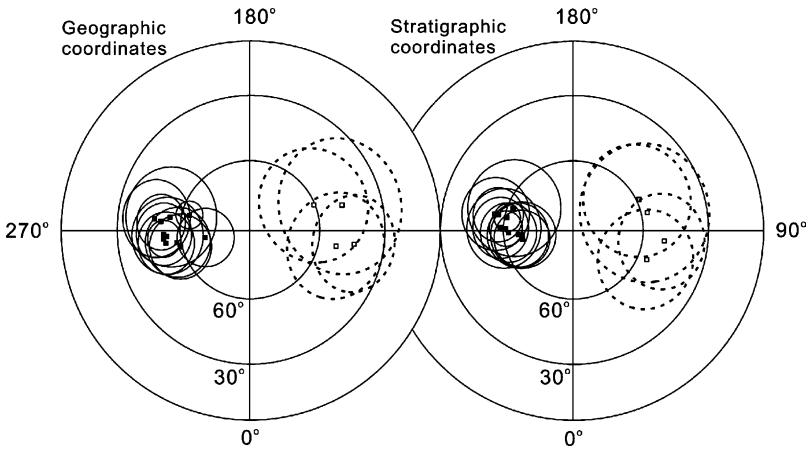

Fig. 7. Distribution of pole positions from site-means of the lower Yunmengshan Formation (for data see Table 2). After tilt correction the data pass a McFadden and McElhinny (1990) reversal test with $\gamma_c = 13.7$, class 'C'.

Fig. 9). In combination with the positive fold test in Member 4, we interpret this component as probably of primary origin. The data are listed in Table 2.

Site YX49 consists of eight samples of purple sandstone at the top of the Yunmengshan Formation. They yielded stable endpoints between 570 and 640 °C, directed shallowly downward toward the NNW (Figs. 5i and 6f). The palaeomagnetic pole calculated from this component overlaps the Triassic palaeopoles for the NCB both before and after tilt-correction (pole B1 in Fig. 10). We thus infer it to be the 'B' component, which is likely a Mesozoic overprint related to collision between the North and South China blocks (Zhang et al., 2000). The data are listed in Table 1.

4.3. Lower Baicaoping Formation

In the Lushan region, samples were collected from a purple mudstone unit in the lower part of the Baicaoping Formation (sites Ls22-Ls24, Fig. 3). NRM intensities are in the range of 1–10 mA m^{-1}. Component 'A' was identified in more than half of the samples below ca. 450 °C, and dominates in a few samples. There is also a high-temperature component directed to the southeast with moderate downward inclination (Figs. 5j and 8a).

Samples from the Ruyang region (sites Ry15-Ry17, Fig. 3) were from purple muddy sandstone. Their NRM intensities are in the order of 1.0 mA m^{-1}. Two remanence components have been identified. Component 'A' is found at low temperatures but sometimes it is stable up to 680 °C (Fig. 5k). The high-temperature component, defined either as vectors or stable endpoints between ca. 500 and 680 °C, has dual polarities (Fig. 5l–m). It is directed either to the northwest and upward or to the southeast and downward with shallow inclination (Fig. 8b).

The high-temperature components from the two study regions group marginally better after structural correction, with the A_{95} of the mean pole decreasing from 13.8 to 11.1 after structural correction (Table 2). Although this mean pole falls close to the palaeopoles of Middle to Late Cambrian and Ordovician ages from the NCB (pole 4 in Fig. 9), considering that there was no Cambrian-Ordovician tectonic event in North China that might have caused a remagnetisation, and that the remanence was probably acquired before folding, we interpret this remanence to be primary (Table 2).

Purple sandstone at the top of the Baicaoping Formation in the Lushan region (site YX50) yielded a high-temperature component directed to the north and downward. This result will be discussed together with those from the Beidajian Formation below.

4.4. The Beidajian Formation and the uppermost part of the Baicaoping Formation

Purple sandstones and purple dolomite were sampled from the Beidajian Formation in the Lushan region. Their NRM intensities range between 1 and 10 mA m^{-1}. Most samples exhibit two components. A soft 'A' component unblocks at about 400 °C and a high-temperature component unblocks between 400 and 640 °C and is directed shallow to the north (Fig. 5n). After tilt correction, the inclinations become steeper. As mentioned in Section 4.3, site YX50 from the uppermost Baicaoping Formation has a similar high-temperature component and is thus considered together with the Beidajian Formation here (Fig. 8c). The pole position of this component after

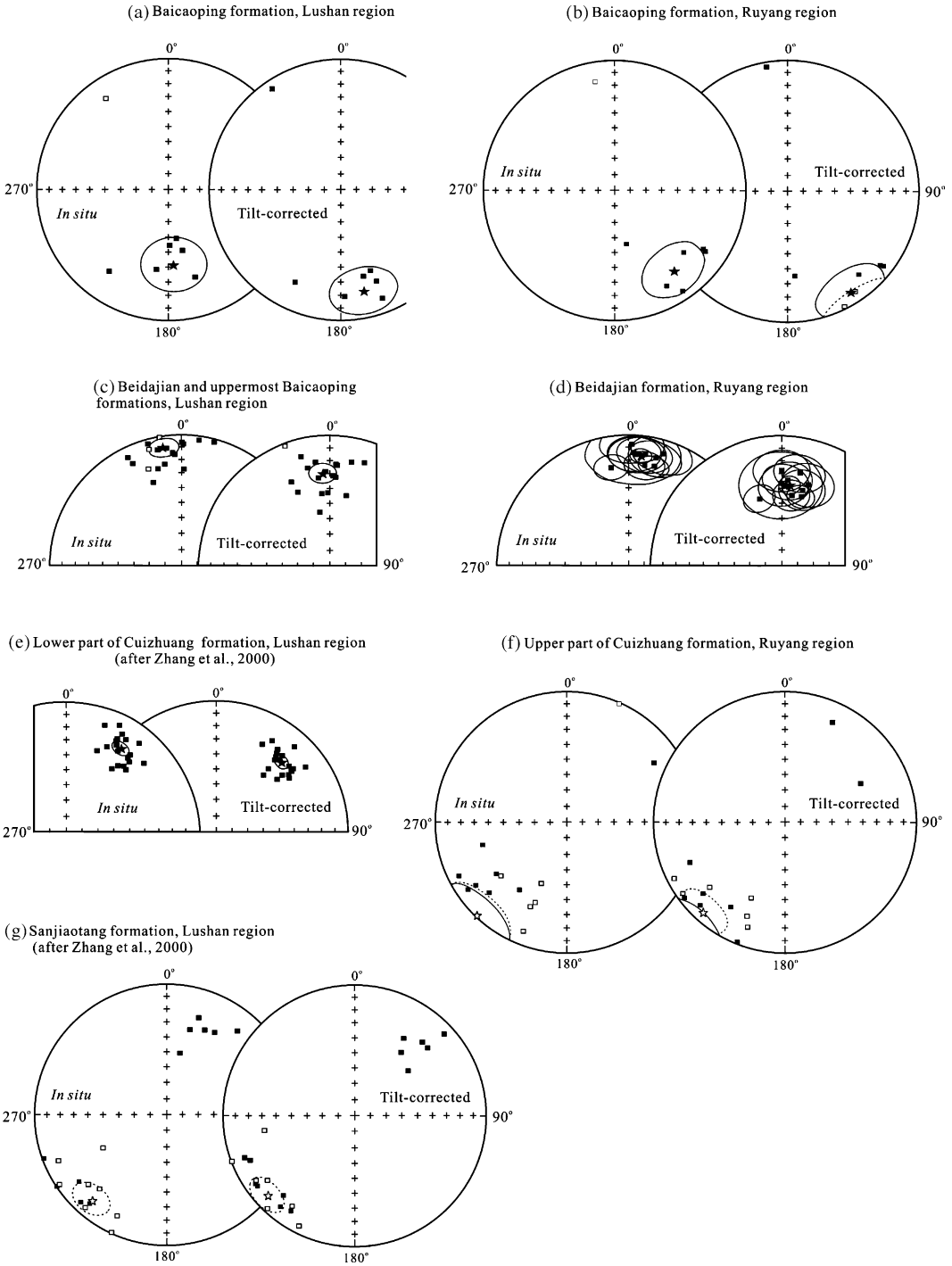

Fig. 8. Stereographic plots of stable remanence directions from the post-Yunmengshan formations. Conventions are as in Fig. 6.

bedding correction falls very close to Jurassic poles of the NCB (pole B2 in Fig. 10), and is thus interpreted to be a 'B' overprint. Similar overprints are also found in Neoproterozoic successions around the NCB, especially in the Xu-Huai region (see Section 5.1.1). These overprints were probably acquired during collision of the South and North China Blocks in the Mesozoic (Zhang et al., 2000).

In the Ruyang region, purple sandstone, muddy sandstone and muddy dolomite were sampled from the Beida-

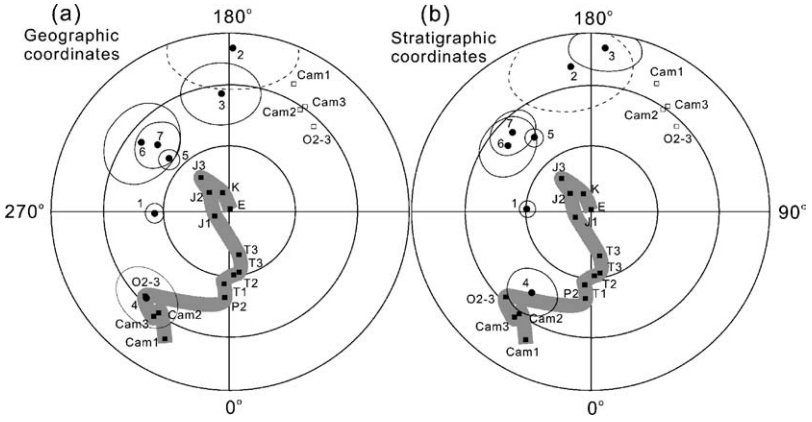

Fig. 9. Interpreted Proterozoic primary poles for the NCB (solid dots, numbers as in Table 2) with 95% confidence circles plotted against known Phanerozoic poles (solid squares) and APWP (after Yang et al., 1998). In (a) the poles are plotted in geographic coordinates, whereas in (b) they are plotted in stratigraphic coordinates. The alternative polarity for the Cambro-Ordovician poles is also shown. Cam1: Early Cambrian; Cam2–3: Middle to Late Cambrian; O1–2: Early to Middle Ordovician; P2: Late Permian; T1: Early Triassic; T2–3: Middle to Late Triassic; J1/J2/J3: Early/Middle/Late Jurassic; K: Cretaceous; E: Tertiary.

jian Formation. Their demagnetisation behaviour resembles those of the same formation in the Lushan region. Most samples have two components. After removing a soft component 'A' by ca. 400 °C, a high-temperature component is revealed between 400 and 640 °C, directed shallowly to the north (Fig. 5o). The site-mean directions resemble those of the Jurassic overprint found in the Beidajian Formation in the Lushan region (Fig. 8c–d), and the corresponding pole after tilt correction falls close to the Middle and Late Jurassic poles for the NCB (pole B3 in Fig. 10b), indicating a Mesozoic overprint.

4.5. New results from Neoproterozoic successions

Neoproterozoic successions in the Ruyang region, including the Cuizhuang, Sanjiaotang and Luoyukou formations, were sampled systemically for palaeomagnetic analysis. Fifteen specimens of purple muddy sandstone from the upper part of the Cuizhuang Formation yielded a stable hard component with unblocking temperatures near 680 °C (Fig. 5p). The directions of the hard component resemble the interpreted primary component from the same formation in the Lushan region (Zhang et al., 2000). The quartz sandstone samples in Sanjiaotang Formation give no stable remenance. We list in Table 2 results of both studies from the Cuizhuang and Sanjiaotang formations, and plot their directions in Fig. 8e–g.

The magnetic behaviour of the purple dolostone samples from the Luoyukou Formation is similar to those from the Lushan region (Zhang et al., 2000). Only overprint components A and B were identified. In most sam-

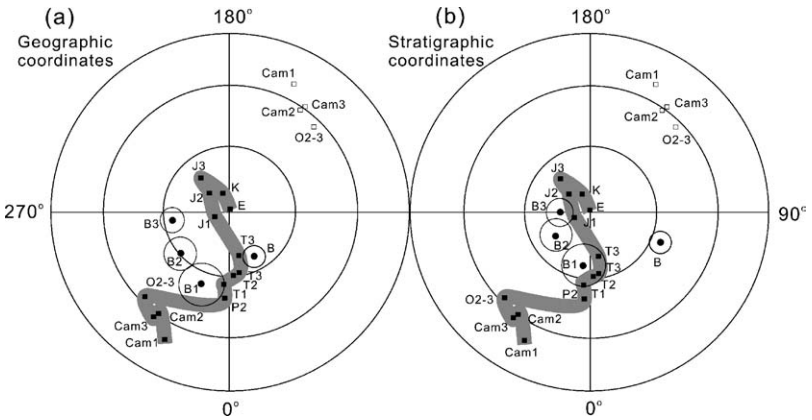

Fig. 10. Interpreted overprint poles (circles) with 95% confidence circles plotted against known Phanerozoic poles (squares) and APWP for the NCB (Phanerozoic APWP connection after Yang et al., 1998). In (a) the poles are plotted in geographic coordinates, whereas in (b) they are plotted in stratigraphic coordinates. Pole B is the Mesozoic overprint after Zhang et al. (2000). Poles B1 to B3 are as in Table 1.

ples, component 'A' could be isolated before 490 °C and component 'B' between 450 and 600 °C. These results are listed in Table 1.

4.6. The origin of remanence

The remanence isolated from the Meso- to Neoproterozoic strata during this study can be classified into three types: a soft component 'A', which is a Recent-field overprint, a 'B' component, acquired during Mesozoic continental collision, and a high-temperature component of probable primary origin.

Component 'A' is found throughout the successions in the two study regions. In some rocks, it dominates the remanence of specimens with unblocking temperatures as high as ∼650 °C, but more commonly it is a soft component coexisting with other components. A few reversed directions of component 'A' are found in both carbonate rocks and purple sandstones. Its directions before tilt correction are close to the Recent field direction, and it is interpreted as a chemical/viscous remanence acquired in Recent time.

Zhang et al. (2000) identified a Mesozoic overprint (component 'B') in this region. It resides pervasively in most Neoproterozoic and Cambrian carbonate rocks, but is rarely seen in purple mudstones or mud-rich dolomite samples. The calculated poles using the in situ directions overlap within error limits with the Triassic poles of the NCB, but not so using the tilt-corrected directions. Component 'B' identified from clastic rocks from the current study (Table 1 and Fig. 10) better resembles the Mesozoic poles after bedding correction (poles B1, B2, B3 in Fig. 10). This indicates that Mesozoic remagnetisation occurred both before and after regional deformation, possibly caused by tectonic fluid migration from the Qinling orogenic belt during Mesozoic orogenesis.

We interpret the remanence listed in Table 2 to be of primary in origin for the following reasons:

(1) All are high-temperature components isolated after removal of a soft component 'A', or an aberrant remanence likely acquired after sampling,
(2) Their corresponding palaeopoles, either in situ or tilt corrected, mostly fall away from known Phanerozoic palaeopoles of the NCB (Fig. 9),
(3) The remanence directions from different stratigraphic units are different from each other, arguing against them being magnetic overprints,
(4) The positive fold test and reversal test in some rock units (opportunities for fold tests are limited owing to the monoclinal attitude of the strata). The age of folding is taken to be the same as the regional tilting, i.e. between 260 and 155 Ma.

However, the quality of the primary palaeomagnetic data varies. Results from the lower Yunmengshan Formation are the most reliable. The remanence is found in 15 sites from two regions over 50 km apart, and has dual polarities. It passes fold and reversal tests. It resides in hematite in redbeds and magnetite in volcanic rocks. Stratigraphically consistent glauconite ages also suggest that no major thermal event has occurred since deposition. The data from the middle and upper parts of the Yunmengshan Formation are the most unreliable owing to small sample numbers.

5. Apparent polar wander path (APWP) and palaeogeographic implications

5.1. Assessment of existing Precambrian palaeomagnetic data from the NCB

To establish the Precambrian APWP for the NCB in light of our new results, we assessed the quality of all available Precambrian palaeomagnetic data from the NCB using the 7-point criteria system of Van der Voo (1990). We list in Table 3 all the poles that have '*Q*' values of 2 or greater.

Many results failed criterion 2 because they were based on less than 25 samples. In three earlier studies, only a portion of the samples was stepwise demagnetised and bulk demagnetisation methods routinely applied, thus failing criterion 3. Most data do not have fold tests or other field tests to satisfy criterion 4. We classified the available poles into three types: (1) Overprint poles, rejected when there is sufficient evidence to suggest an overprint origin; (2) Questionable poles, when poles from the same stratigraphic unit by different authors contradict each other and there is no strong reason to suggest one of them as primary; data of questionable quality have not been used for the palaeocontinental reconstructions in this paper; (3) Accepted poles, results that we regard as reliable based on their *Q*-values.

5.1.1. Late Neoproterozoic (ca. 800–542 Ma)

There are 26 poles for this time interval. Although all are inferred to be of primary origin by the original authors, we suggest that many are not (Table 3). The rejected poles include those from 12 rock units in the Xu-Huai region (Fig. 1) that cover a period of ca. 200 Ma. Their tilt-corrected magnetic remanence directions are indistinguishable from one another. Piper and Zhang (1997) reported such a remanence from the Feng-

Table 3
Selected Meso- to Neoproterozoic palaeomagnetic poles from the North China Block

No.	Rock unit, sampling area	*n*(*N*)	Plat (°N)	Plon (°E)	dp/dm A_{95} (°)	Quality criteria							*Q*	Comment	Mean pole	Age (Ma)	Ref.
						1	2	3	4	5	6	7					
"Sinian" (~800–542 Ma)																	
1	Jinshanzhai Fm, Xu-Huai	4	76.0	256.7	2.1/3.5	+				+			2	Overprint			1
2	Dongjia Fm, Lushan	26	−60.8	97.4	4.3/8.5	+	+	+		+	+	+	6	Accepted	*DJ*	650	2
3	WangshanFm, Xu-Huai	28	74.8	253.0	11.0/18.0	+	+			+			3	Overprint			1
4	Shijia Fm, Xu-Huai	14	77.1	279.8	7.3/12.0	+				+			2	Overprint			1
5	Weiji Fm, Xu-Huai	23	57.1	195.2	29.0/42.0	+				+			2	Overprint			1
6	Zhangqu Fm, Xu-Huai	11	−46.4	108.7	4.5/8.6	+				+			2	Accepted			1
7	Jiudingshan Fm, Xu-Huai	10	61.4	234.1	16.6/29.2	+				+			2	Overprint			1
8	Jiudingshan Fm, Xu-Huai	6	68.0	227.0	–	+				+			2	Overprint			1
9	Niyuan Fm, Xu-Huai	6	−44.0	114.3	4.9/9.3	+				+			2	Accepted			1
10	Niyuan Fm, Xu-Huai	15	67.0	210.0	–	+				+			2	Overprint			1
11	Ganjingzi Fm, Fuzhou	14	65.7	169.3	11.6/13.8	+				+			2	Overprint			3
12	Nanguanling Fm, Fuzhou	12	60.0	219.0	8.3/12.5	+				+			2	Overprint			3
13	Changlingzi Fm, Fuzhou	19	47.0	166.0	21.5/24.3	+				+			2	Questionable			3
14	Zhaowei Fm, Xu-Huai	10	−41.2	101.7	13.0/24.7	+				+			2	Accepted			1
15	Jiayuan Fm[a], Xu-Huai	8	−39.7	104.0	11.9/21.7	+				+			2	Accepted			1
	Average Poles 6,9,14,15		−42.9	107.0	5.7										*HB*	700	
16	Jushan Fm, Xu-Huai	18	82.5	182.5	11.4/16.7	+				+			2	Overprint			1
17	Qiaotou Fm, Fuzhou	4	−34.3	356.6	11.7/14.6	+				+			2	Questionable			3
18	Nanfen Fm, Fuzhou	14	63.9	161.8	5.9/10.2	+				+			2	Overprint			3
19	*Nanfen Fm, Fuzhou*	57(8)	−16.5	121.1	8.8/13.0	+	+	+		+		+	5	Accepted	*NF*	800–780	4
20	Diaoyutai Fm, Fuzhou	22(2)	61.0	239.0	11.0	+				+			2	Overprint			5
21	Xinxing Fm, Xu-Huai	35(7)	65.4	175.1	17.0/22.0	+	+			+			3	Overprint			1
22	Lanling Fm, Xu-Huai	5(2)	69.4	242.2	12.4/21.0	+				+			2	Overprint			1
23	Jiuliqiao Fm, Xu-Huai	4	64.0	169.0	–	+				+			2	Overprint			1
24	ShouxianFm, Xu-Huai	11	65.0	185.0	–	+				+			2	Overprint			1
25	Liulaobei Fm, Xu-Huai	19	42.6	149.6	11.9/13.0	+		+		+		+	4	Questionable			6
26	Liulaobei Fm, Xu-Huai	18	61.0	182.0	–	+				+			2	Overprint			1
Qingbaikouan (~1000–800 Ma)																	
27	Red beds, U. Jingeryu Fm, Jixian	15	3.8	142.7	6.1/7.6	+		+		+		+	4	Questionable			7
28	Grey rocks, L. Jingeryu Fm, Jixian	13	−12.5	170.3	8.6/15.2	+		+		+		+	4	Questionable			7
29	Red beds, U. Jingeryu Fm, Jixian	6	−49.9	94.4	8.1/16.2	+		+		+		+	4	Questionable			7
30	Red beds, U. Jingeryu Fm, Jixian	4	−54.4	101.5	13.1/25.9	+		+		+		+	4	Questionable			7
31	Jingeryu Fm, Jixian	16(2)	67.0	132.0	23.3/25.6	+				+			2	Overprint			5
32	Changlongshan Fm, Jixian	24(3)	60.0	243.0	15.9/27.7	+				+			2	Overprint			8
33	Xiamaling Fm, Jixian	29(2)	29.0	200.0	21.0/34.9	+				+			2	Overprint			5
34	Xiamaling Fm, Jixian	9	−23.1	209.7	6.2/11.0	+		+		+		+	4	Questionable			7
35	*Sanjiaotang Fm, Lushan*	20	−35.9	44.4	5.1/10.1	+		+		+	+	+	5	Accepted			2
36	*U. Cuizhuang Fm, Ruyang*	14	−40.0	51.4	6.7/13.4	+		+		+	+	+	5	Accepted			0
37	*L. Cuizhauang Fm, Lushan*	19	−46.6	37.8	2.5/4.6	+		+		+		+	4	Accepted			2
	Average poles 35,36,37		−41.0	44.8	11.3	+	+	+		+	+	+	6		*CS*	950	

Jixianian (~1400–1000 Ma)																	
38	Tieling Fm, Jixian	7	12.9	188.4	3.3/5.6	+		+		+		+	4	Accepted			9
39	Tieling Fm, Jixian	9	15.6	178.3	5.3/7.9	+		+		+		+	4	Accepted			9
40	Tieling Fm, Jixian	5	33.0	195.6	11.5/17.6	+		+		+		+	4	Accepted			9
41	Tieling Fm, Jixian	5	−21.3	167.9	3.6/6.8	+		+		+		+	4	Accepted			9
42	Tieling Fm, Jixian	4	−20.5	126.2	29.7/45.5	+		+		+		+	4	Accepted			9
43	Tieling Fm, Jixian	4	−8.1	138.9	23.2/31.7	+		+		+		+	4	Accepted			9
44	Tieling Fm, Jixian	6	−6.0	103.4	14.5/18.9	+		+		+		+	4	Accepted			9
45	Tieling Fm, Jixian	6	8.2	128.5	24.4/27.8	+		+		+		+	4	Accepted			9
46	Tieling Fm, Jixian	6	−7.3	153.1	18.6/27.3	+		+		+		+	4	Accepted			9
47	U. Tieling Fm, Jixian	8	−9.4	217.5	11.2/20.7	+		+		+		+	4	Accepted			7
48	L. Tieling Fm, Jixian	10	24.0	207.5	5.7/10.3	+		+		+		+	4	Accepted			7
	Average poles 38–48		2.2	163.6	25.3	+	+	+		+		+	5		*TL*	1100	
49	Tieling Fm, Jixian	34(4)	−67.0	84.0	30.0	+				+			2	Overprint			5
50	Hongshuizhuang Fm, Jixian	19(3)	47.0	322.0	20.0	+				+		+	3	Questionable			5
51	Hongshuizhuang Fm, Jixian	6	39.4	161.4	10.4/11.9	+		+		+		+	4	Questionable			9
52	Hongshuizhuang Fm, Jixian	6	28.8	171.4	10.1/12.8	+		+		+		+	4	Questionable			9
53	Wumishan Fm, Jixian	6	7.6	135.4	29.1/33.9	+		+		+		+	4	Questionable			9
54	Wumishan Fm, Jixian	3	32.1	173.3	32.6/41.5	+		+		+		+	4	Questionable			9
55	Wumishan Fm, Jixian	15	−18.2	49.2	5.4/10.7	+		+		+		+	4	Accepted			7
56	Wumishan Fm, Jixian[b]	81(9)	−16.7	43.4	17.0	+	+			+			3	Accepted			5
57	Yangzhuang Fm, Jixian	48(6)	−17.0	246.0	12.0	+	+			+			3	Overprint			5
58	Yangzhuang Fm, Jixian	62(4)	−16.5	42.5	12.8/25.6	+	+	+		+	+	+	6	Accepted			7
	Average poles 55,56,58		−17.2	45.0	5.5										*JXA*	1300	
59	*Baicaoping Fm, Lushan and Ruyang*	14	−43.0	143.8	11.1	+		+		+			3	Accepted	*BCP*	1200	0
60	*Mb 3, Yunmengshan Fm, Lushan*	9	−19.0	188.5	11.6/23.1	+		+		+		+	4	Less reliable			0
61	*Mb 4, Yunmengshan Fm, Lushan*	10	9.2	175.4	10.5/16.4	+		+	+	+		+	5	Less reliable			0
62	*Mb 1,2 Yunmengshan Fm, Lushan and Ruyang*	108(15)	−60.6	87.0	3.7	+	+	+	+	+	+	+	7	Accepted	*YMSL*	1260	0

Geographic coordinates of major field regions: Lushan (33.8°N, 112.6°E); Ruyang (34.25°N; 112.5°E); Jixian (40.2°N, 117.3°E); Fuzhou (41.3°N, 123.7°E); Xu-Huai (32.5–35.0°N; 116.5–117.5°E). Abbreviations for rock units: Mb, Member; Fm, Formation; Gp, Group; U., upper part; L., lower part. $n(N)$: sample number (site number). Quality Criteria and Q values (number of criteria met) after Van der Voo (1990): 1, well determined rock age; 2, sufficient number of samples, $n > 24$, k (or K) ≥ 10, $\alpha_{95} \leq 16.0°$; 3, step-wise demagnetization; 4, field tests; 5, structural control and tectonic coherence with the craton discussed; 6, presence of reversal; 7, no resemblance to paleopole of younger age (by more than a period). Poles used for defining the APWP are listed under "Mean Pole". Ages for poles are according to data in Fig. 4. Reference (Ref.): 0, this study; 1, Fang et al. (1983); 2, Zhang et al. (2000); 3, Gao and Fan (1983); 4, Lin (1984); 5, Zhang and Zhang (1985); 6, Piper and Zhang (1997); 7, Zhang et al. (1991); 8, Zhang and Li (1980); 9, Lin (1988). Other abbreviations are the same as in Table 1.

[a] The Jiayuan Formation has been combined with the lower member of the Jiuliqiao Formation (Xing, 1989).

[b] The pole was recalculated using the directional data.

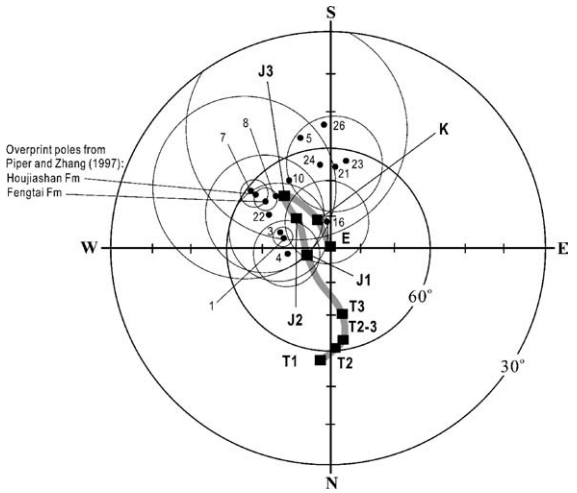

Fig. 11. Possible Late Mesozoic–Cenozoic remagnetization poles (small dots) identified from Precambrian rock units in the Xu-Huai region, NCB, plotted against the Mesozoic–Cenozoic APWP (after Yang et al., 1998). For age symbols see Fig. 9. Poles are numbered as in Table 3.

tai Formation in the same region, and referred to it as a Cambrian remagnetization because the remanence also exists in the overlying Cambrian strata. However, the corresponding poles do not agree with the known Cambrian poles in Zhao et al. (1996) and Huang et al. (1999), but overlap with the Jurassic-Cretaceous poles of the NCB within error limits (poles 1, 3–5, 7, 8, 10, 16, 21–24, 26 in Fig. 11). Poles 11, 12, 18, 20 from the "Sinian" strata in Fuzhou, and poles based on component 'B' of the current study, also fall close to younger pole positions. We thus suggest that the overprints were acquired in the Mesozoic during collision of the North and South China Blocks.

Poles 13 and 17 (Table 3) are questionable because of their lack of verifiable details. Pole 25 was identified from red shale in the lower part of the Liulaobei Formation, an isolated outcrop in the Xuhuai region. This red shale is also called the Guanjiaying Formation and is correlated with the Nanfen Formation in the Fuzhou region (e.g. Xing, 1989) (Fig. 4). However, palaeomagnetic results from the two localities are quite different. Pole 25 predicts a palaeolatitude of 62° for the Xuhuai region, 22° higher than that predicted by pole 19. There is also a ∼115° difference in implied palaeo-azimuths. Palaeolatitudes above 60° is not favourable for development of red shale and carbonate in the two formations. We thus choose to use pole 19 rather than 25 for the two formations.

The accepted results (poles 2, 6, 9, 14, 15 and 19 in Table 3) fall close to the Cambrian poles and indicate that the NCB occupied lower latitudes in the late Neoproterozoic (Fig. 12). This is consistent with the low-latitude lithological indicators such as redbeds, carbonate and storm deposits. Because poles 6, 9, 14, 15 were all from the Huaibei group in the Xu-Huai region (Fig. 1) and agree with each other, they are combined as Pole 'HB' here.

5.1.2. Early Neoproterozoic (ca. 1000–800 Ma)

There are 11 poles from early Neoproterozoic (Qingbaikouan) interval (Table 3). Poles 27–30, by Zhang et al. (1991), are all from the Jingeryu Formation. Without any evidence for the reliability of these vastly different poles, we regard them as questionable. Poles 31, 32, 33 were reinterpreted by Lin (1988) as Recent overprints because their in situ directions are similar to Recent field direction. Pole 34 was based on demagnetisation curves that fail to reveal stable remanence directions (see Zhang et al., 1991, Figs. 2-2, 4 and Table 2), and is thus a questionable pole. Pole 28 was based on 13 samples only. Poles 35–37 cannot be regarded as reliable on individual basis, but the three poles from adjacent stratigraphic units agree very well. We thus average them to give a mean pole (pole "CS" in Table 3).

5.1.3. Late Mesoproterozoic (ca. 1400–1000 Ma)

Palaeomagnetic data for late Mesoproterozoic (Jixianian) time are from Jixian, Hebei Province, and western Henan Province (Positions 2 and 4, Fig. 1). Stratigraphic correlations between rock units of the two regions is given in Fig. 4.

Twelve polaeopoles were reported from the Tieling Formation, (poles 38–49, Table 3). The first eleven were acquired using modern palaeomagnetic technology, but the sample number for each pole is small (between 4 and 10), and the poles exhibit large scatter. We calculated a mean of the 11 poles to be representative of this formation (pole "TL", Table 3). Pole 49 falls far from the other Tieling Formation results but near the area of Mesozoic overprint poles. In addition, samples for pole 49 were only partially demagnetised. This pole is thus unreliable.

Three poles have been reported from the Hongshuizhuang Formation (poles 50–52). Pole 50 is significantly different from the other two. Lin (1988) suggested that the remanence used for pole 50 was contaminated by secondary components. Poles 51 and 52 were based on only six samples each, and are thus not sufficiently reliable.

The Yangzhuang and Wumishan formations have thicknesses of 707 and 3336 m respectively, with the for-

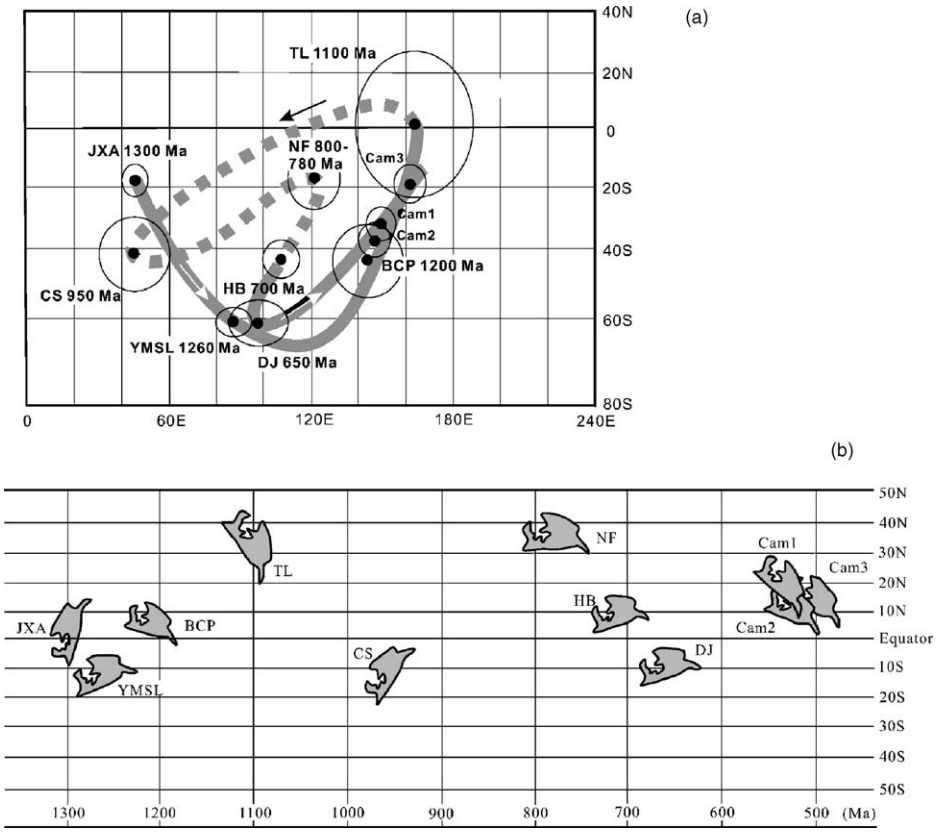

Fig. 12. (a) Preliminary APWP for the NCB between ca. 1300 and 500 Ma. For abbreviations of Precambrian pole see Table 3. The Cambrian poles are after Huang et al. (1999) but with a reversed polarity (Zhao et al., 1996). Dashed section of the APWP is least-well constrained. (b) Paleo-latitude and orientation of the NCB implied by the APWP. Mercator projection.

mer consisting of mainly grey to purplish red muddy dolostone and siltstone, and the latter of cyclic carbonate and clastic rocks with minor redbeds in the middle part of the formation. Data from the Wumishan Formation (poles 53–56), reported by Lin (1988) and Zhang et al. (1991), are significantly different from each other. We regard poles 55 and 56 as more reliable because they were based on significantly larger numbers of samples, whereas poles 53 and 54 are questionable because of their small sample numbers and large uncertainties.

Pole 57 from the Yangzhuang Fm was inferred by Lin (1988) to be an overprint because of the similarity of its in situ direction to Mesozoic directions, whereas pole 58 meets all the reliability criteria apart from a fold test. It falls close to poles 55 and 56 from the redbed unit in the middle part of the overlying Wumishan Formation, all being clearly removed from known younger pole positions. We averaged these three poles as mean pole 'JXA' (Table 3).

5.2. *Preliminary APWP and palaeolatitude of the North China Block between ~1300 and 500 Ma*

Using the 25 accepted datasets out of the total of 62 in Table 3, we calculated eight representative poles for Meso- and Neoproterozoic rocks of the NCB. Due to the lack of reliable isotopic ages from these sedimentary successions, assigning ages to these poles is difficult. In Table 3 we give estimated ages based on age information and regional stratigraphic correlations as in Fig. 4 (see further discussions below). We note the tentative nature of these ages, but emphasise the stratigraphic order following which we connect the palaeopoles into a preliminary APWP.

Pole DJ is assigned an age of ~650 Ma based on the glauconite K–Ar age of the Dongjia Formation (Fig. 4). Pole HB is assigned an age of ~700 Ma according to the glauconite K–Ar ages for the Zhaowei Formation (738 Ma, Fang et al., 1983) and the Shijia Formation (681 Ma, Fang et al., 1983; Xing, 1989) in the Huaibei

Group. In the Fuzhou region, the Nanfen Formation is correlated with the uppermost part of the Qingbaikouan (ca. 1000–800 Ma), and has a glauconite K–Ar age of 787 Ma. We thus bracket its age as ~800–780 Ma. Isotopic ages for the Cuizhuang and Sanjiaotang formations are in the range of 990–1160 Ma. However, many researchers correlate these units with the Qingbaikouan Xiamaling Formation in the Jixian stratotype section, which has a glauconite K–Ar age of 956 Ma (Xing, 1989) and a limestone Pb–Pb age of 879 ± 18 Ma (Qiao and Gao, 1997). Furthermore, there is a Pb–Pb age of 855 ± 54 Ma from the Luoyukou Formation (Fig. 4) which conformably overlies the Sanjiaotang Formation. We thus assigned an age of ~ 950 Ma to the Cuizhuang and Sanjiaotang formations. Variations in glauconite K–Ar ages from the Tieling Formation is over 200 million years with an average of ca. 1100 Ma. An age of ~1270–1100 Ma for the Ruyang Group is consistent with both the isotopic ages and the stratigraphic correlation with the Jixian section (Xing, 1989; Fig. 4). Pole BCP from the middle Ruyang Group is therefore assigned an age around 1200 Ma. Pole YMSL, from the basal units, which satisfies all the seven quality criteria with an age of ~1270 Ma, is one of the most reliable poles for the Precambrian NCB. Pole JXA is an averaged pole for Wumishan and Yangzhuang formations, which are the lowest rock units in the Jixianian section. An estimated age of ~1300 Ma is given to this pole, based on isotopic data (Fig. 4) and stratigraphic position.

Fig. 12a shows a preliminary APWP for the NCB from ca. 1300 Ma to the Cambrian. We applied the rule of maintaining a minimal distance between two consecutive poles in constructing the APWP, except for the case of poles TL and CS, where we reversed the post-1100 Ma poles in order to match the APWP of Laurentia (see discussions in the following section). In doing so we adapted the polarity of Zhao et al. (1992, 1996) for the Cambrian poles (polarity option 1 hereafter). This is opposite to the polarity given by other workers (e.g. Lin et al., 1985; Huang et al., 1999), which we call polarity option 2 hereafter. Fig. 12b shows the palaeolatitudes and orientations of the NCB implied by the APWP option 1. It demonstrates that North China remained at low to intermedium palaeolatitudes from ca. 1300 Ma to early Palaeozoic. Given the uncertainty in the polarities, NCB could also have been at mirror image positions to those shown in Fig. 12b relative to the equator.

5.3. North China's position in Rodinia

In testing configurations of the Late Precambrian supercontinent Rodinia, Precambrian palaeomagnetic data worldwide have been comprehensively reviewed (e.g. Powell et al., 1993; Torsvik et al., 1996; Smethurst et al., 1998; Weil et al., 1998; Buchan et al., 2000, 2001; McElhinny and McFadden, 2000; Meert and Powell, 2001; Pisarevsky et al., 2003; Pisarevsky and Natapov, 2003). Laurentia, as a central piece in Rodinia reconstructions and with the best-established Late Precambrian APWP, provides a good reference for testing whether the NCB was part of Rodinia.

Buchan et al. (2001) selected more than a dozen key poles for Precambrian Laurentia. They fall in the intervals of ca. 1460–1420, 1270–1230, 1140–1090 and 780–720 Ma. Together with the Grenvillian overprint poles related to the Grenville orogeny, two APWP loops have been identified for Laurentia (Fig. 13). The older Logan Loop, a counter clockwise loop between 1460 and 1087 Ma (the Logan loop), is well defined by key poles (Buchan et al., 2001). However, the subsequent Grenville Loop, between ca. 1050 and 720 Ma, is defined by both key poles and overprint poles, and its trend is still under debate (e.g. Weil et al., 1998; McElhinny and McFadden, 2000). In this study, we adapt the clockwise Grenville loop following some recent work (e.g. Alvarez and Dunlop, 1998; McElhinny and McFadden, 2000; Pisarevsky et al., 2003), notwithstanding that the alternative counter-clockwise loop (e.g. Weil et al., 1998) cannot be ruled out.

Fig. 13 presents a possible position of the NCB in Rodinia by matching its APWP with the APWP of Laurentia (Euler rotation of NCB relative to Laurentia: 39°N, 87°E, 74° counter clockwise). In this configuration, palaeopoles from the two continents match relatively well between ca. 1250 and ca. 700 Ma (Fig. 13): the ca. 1200 Ma BCP pole of the NCB falls between the ca. 1270 Ma poles and the 1100 Ma poles for Laurentia; the TL pole of the NCB overlaps the ca. 1100 Ma Laurentian poles; the ca. 950 Ma CS pole overlaps the ca. 980 Ma pole from the Hailiburton Intrusion in Grenville Belt; the ca. 800–780 Ma NF pole and the ca. 700 Ma HB pole of the NCB fall close to the 780 Ma and 723 Ma poles from Laurentia. The correspondence of 800–700 Ma poles is not as close as for the older poles, which may be due partly to true polar wander, as suggested by Li et al. (2004) for that time interval.

The position of the NCB relative to Laurentia in Fig. 13 is similar to that suggested by Li et al. (1996), but with a modified orientation. There is a ca. 3000 km gap between the NCB and Laurentia in this fit, which can accommodate the Siberia craton (e.g. Hoffman, 1991; Condie and Rosen, 1994; Frost et al., 1998; Rainbird et al., 1998; Pisarevsky et al., 2000), or possibly other continental blocks. In Fig. 13 we have

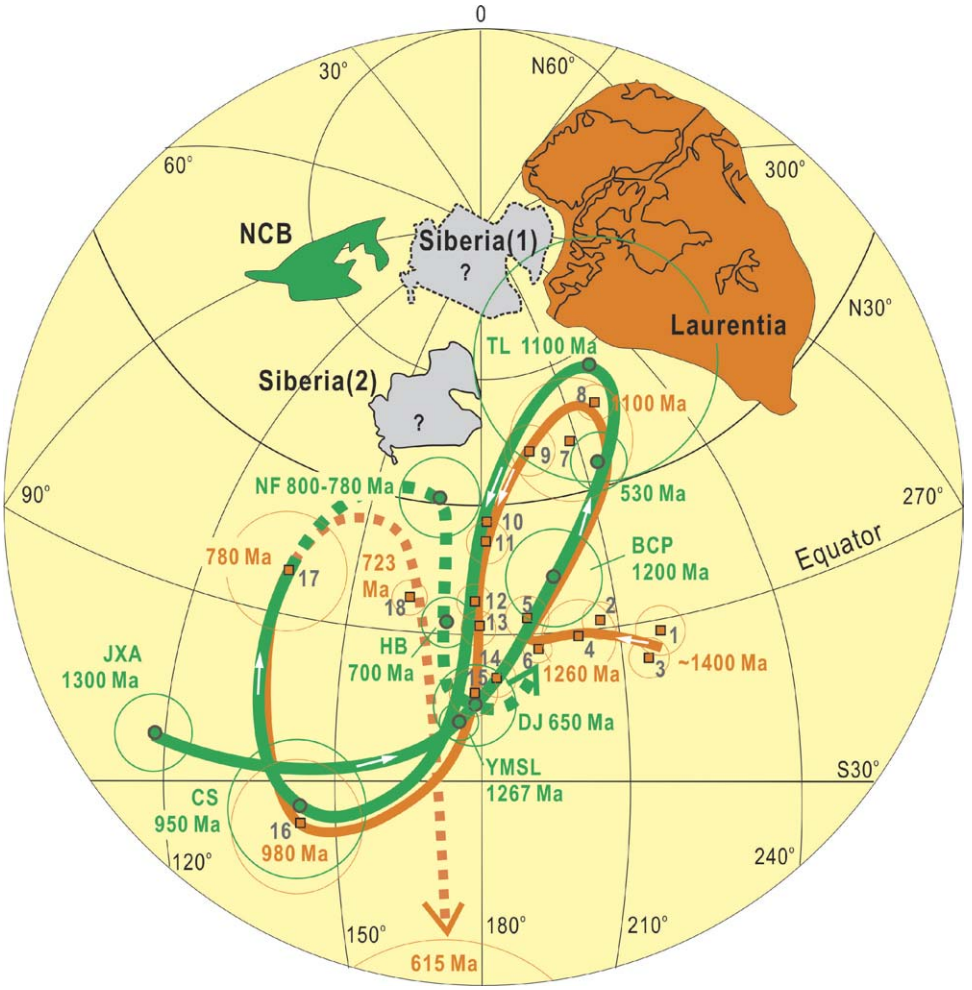

Fig. 13. Relationship between the NCB and Laurentia based on the best fit of the palaeomagnetic data (all in present North America coordinates). NCB poles (green dots; Table 3) are plotted with their A_{95} (95% confidence circles), after being rotated to North America using Euler rotation (39°N, 087°E, 74°). Key Laurentian poles (orange squares; Buchan et al., 2001, Table 1) are numbered and shown as small squares: 1. Michikamau anorthosite pluton, 1460 Ma; 2. Harp Lake complex, 1450 Ma; 3. Laramie complex and Sherman Granite, 1434 Ma; 4. Mistastin complex, 1420 Ma; 5. Mackenzie dolerite dykes, 1267 ± 2 Ma; 6. Sudbury dolerite dykes, 1235 Ma; 7. Abitibi dolerite dykes, 1141 ± 1 Ma; 8. Logan dolerite sills, 1108 ± 1 Ma; 9. Reversely magnetized Upper Osler lavas, 1105 ± 2 Ma; 10. Portage Lake lavas, 1095 ± 3 Ma; 11. Lake Shore traps, 1087 ± 2 Ma; 17. Western North America intrusions, 780 Ma; 18. Franklin dykes, 723 + 4/−3 Ma; other poles of Grenville age are after McElhinny and McFadden (2000) and Pisarevsky et al. (2003): 12. Nonesuch Shale, 1050 Ma; 13. Freda sandstone, 1050 Ma; 14. Jacobsville sandstone, 1020 Ma, 15. Chequamegon Sandstone, 1020 Ma, 16. Hailiburton Intrusion, ∼980 Ma. The 615 Ma Cambrian pole is after Torsvik et al. (1996). Two positions for Siberia are shown: the position in dashed-line (position 1) is after Frost et al. (1998), and the position in solid-line (position 2) corresponds to the best paleomagnetic fit position by Pisarevsky and Natapov (2003). Wulf equal-angle projection.

shown the Siberia-Laurentia fit according to Frost et al. (1998); (position 1) as well as the latest fit by Pisarevsky and Natapov (2003); (position 2). A continental connection between the NCB and Laurentia is consistent with biogeographical analyses of Wang et al. (1997). They found that the 900–800 Ma Tawuia-Longfengshania macroalgae assemblage is almost identical to that found in the Greyson shale in Montana and in the Little Dal Formation in the McKenzie Mountains of northwestern Laurentia, indicating a close relationship between the two continents during the Meso- and Neoproterozoic (Wang et al., 1997; Wang and Zhang, 2002).

The ca. 1270 Ma YMSL pole and the ca. 1300 Ma JXA pole for the NCB are distant from the ca. 1400 to 1260 Ma poles for Laurentia, implying that the NCB probably did not move as a coherent plate with Laurentia before ca. 1200 Ma. The DJ pole from the NCB (ca. 650 Ma) still falls close to the Laurentian APWP (Fig. 13), but not the ca. 530 Ma Early Cambrian pole.

This may indicate that break up between Laurentia and the NCB took place between 650 and 615 Ma.

6. Conclusions

We report here a series of palaeomagnetic poles from thick late Mesoproterozoic to Neoproterozoic successions in the southern North China Block (NCB). Characteristic remanences were isolated after removing a Recent geomagnetic field component and in some units, a Mesozoic overprint. Data from some formations passed fold and/or reversal tests, and the primary origin of their magnetisations is supported by their lack of similarity to any known younger direction, and changes in the remanent directions from different stratigraphic units. Combining our new results with a critical selection of existing data, we established a preliminary apparent polar wander path (APWP) for the NCB between 1300 and 510 Ma. Comparison of the NCB data with those for Laurentia suggests that (1) the NCB moved independently of Laurentia before ca. 1200 Ma, (2) the NCB shared a similar APWP with Laurentia between ca. 1200 and ca. 700 Ma, suggesting that the NCB was part of the supercontinent Rodinia, and (3) the indirect connection between NCB and Laurentia was broken between ca. 650 and 615 Ma.

We note the high uncertainty in the polarity choice for the NCB poles, as well as the uncertainty in the trend of the Grenville loop for Laurentia, both making the reconstruction shown in Fig. 13 tenuous. Furthermore, the relative positions of Siberia and Laurentia are uncertain owing to the lack of high-quality palaeomagnetic poles. To improve the APWP for the NCB, other Precambrian successions in North China need to be systematically studied, and precise isotopic ages need to be obtained from the strata. A reliable reconstruction of NCB, Siberia and Laurentia will require additional high-quality palaeomagnetic data from all three cratons.

Acknowledgements

This study was jointly supported by the National Natural Science Foundation of China (grants no. 49872076, 40032010-B and 59810761886) and Program for New Century Excellent Talents University NCET-04-0727, the ARC Tectonics Special Research Centre (TSRC) grants, and a grant from the University of Western Australia's International Centre. We thank Prof. Z.Q. Lao and Messrs. R.H. Hu, Y.S. Zou, and H. Zhang for their helps during the field trips. Thanks are also given to Profs. D. Jones and H. Wang for discussions, Mr. S. Adams for assistance in the Palaeomagnetism Laboratory at UWA, and Drs. J.E. Glover, S.A. Pisarevsky, M.T.D. Wingate and two reviewers for helpful comments. This is TSRC publication #317, and a contribution to IGCP 440: Rodinia Assembly and Breakup.

References

Alvarez, V.C., Dunlop, D.J., 1998. A regional paleomagnetic study of lithotectonic domains in the Central Gneiss Belt, Grenville Province, Ontario. Earth Planet. Sci. Lett. 157, 89–103.

BGHNP (Bureau of Geology and Mineral Resources of Henan Province), 1989. Regional Geology of Henan Province. Geological Memoirs, People's Republic of China Ministry of Geology and Mineral Resources, Series 1(17), Geological Publishing House, Beijing, pp. 94–124 (in Chinese with English abstract).

Buchan, K.L., Ernst, R.E., Hamilton, M.A., Mertanen, S., Pesonen, L.J., Elming, S.-A., 2001. Rodinia: the evidence from integrated palaeomagnetism and U–Pb geochronology. Precambrian Res. 110, 9–32.

Buchan, K.L., Mertanen, S., Park, R.G., Pesonen, L.J., Elming, S.-A., Abrahamsen, N., Bylund, G., 2000. Comparing the drift of Laurentia and Baltica in the Proterozoic: the importance of key paleomagnetic poles. Tectonophysics 319, 167–198.

Chumakov, N.M., Elston, D.P., 1989. The paradox of Late Proterozoic glaciations at low latitudes. Episodes 12, 115–120.

Condie, K.C., Rosen, O.M., 1994. Laurentia-Siberia connection revisited. Geology 22, 168–170.

Enkin, R.J., Yang, Z.Y., Chen, Y., Courtillot, V., 1992. Paleomagnetic constraints on the geodynamic history of China from the Permian to the present. J. Geophys. Res. 97, 13953–13989.

Fang, D.J., Zhu, Z.W., Guo, Y.B., 1983. Study on the paleomagnetism of Upper Precambrian in Northern Jiangsu and correlation between the Upper Precambrian strata in South and North China. Sci. Geol. Sin. 4, 324–336 (in Chinese with English abstract).

Frost, B.R., Avchenko, O.V., Chamberlain, K.R., Frost, C.D., 1998. Evidence for extensive Proterozoic remobilization of the Aldan shield and implications for Proterozoic plate tectonic reconstructions of Siberia and Laurentia. Precambrian Res. 89, 1–23.

Gao, R.F., Fan, Y.Q., 1983. A Preliminary study of paleomagnetism for Late Precambrian Southern Liaodong Peninsula. Bull. Shenyang Inst. Geol. Min. Res. 6, 122–140 (in Chinese).

Guan, B., Geng, W., Rong, Z., Du, H., 1983. On the age of Luoquan formation in Henan Province. Precamb. Geol. 1, 183–197 (in Chinese with English abstract).

Guan, B., Pan, Z., Geng, W., Rong, Z., Du, H., 1980. Sinian Suberathem in the northern slope of eastern Qinling ranges. In: Tianjin Institute of Geology, Minerals (Ed.), Sinian Suberathem in China, Research on Precambrian Geology. Tianjin Science and Technology Press, Tianjin, pp. 288–311 (in Chinese with English abstract).

Halls, H.C., Li, J., Davis, D., Hou, G., Zhang, B., Qian, X., 2000. A precisely dated Proterozoic paleomagnetic pole from the North China craton, and its relevance to paleocontinental reconstruction. Geophys. J. Int. 143, 185–203.

Hoffman, P.F., 1991. Did the breakout of Laurentia turn Gondwanaland inside-out? Science 252, 1409–1412.

Huang, B., Yang, Z., Otofuji, Y., Zhu, R., 1999. Early Paleozoic paleomagnetic poles from the western part of the North China Block and their implications. Tectonophysics 308, 377–402.

Kirschvink, J.L., 1980. The least-squares line and plane and the analysis of paleomagnetic data. Geophys. J. R. Astron. Soc. 62, 699–718.

Li, C., Wang, Q., Liu, X., Tang, Y., 1982. Explanatory Notes to the Tectonic Map of Asia. Cartographic Publishing House, Beijing, 49 pp.

Li, H., Li, H., Lu, S., 1995. Grain zircon U–Pb ages for volcanic rocks from Tuanshanzi Formation of Changcheng System and their geological implications. Geochimica 24, 43–48 (in Chinese with English abstract).

Li, Q.Z., Yang, Y.Z., Jia, J.C., 1985. The age and sedimentary facies of the Luoquan Formation in the south margin of the North China Platform (the part in Shaanxi Province). In: Precambrian Geology Committee (Eds.), The Collected Work on the Late Precambrian Glaciogenic Rocks of China. Precambrian Geology No. 1, Geology Publishing House, Beijing, pp. 163–182 (in Chinese with English abstract).

Li, S., Hart, S.R., Zheng, S.G., Liu, D., Zhang, G., Guo, A., 1989. Timing of collision between the North and South China Blocks—Sm–Nd isotopic age evidence. Sci. Chin. (Ser. B) 32, 1391–1400.

Li, Z.X., 1998. Tectonic history of the major East Asian lithospheric blocks since the Mid-Proterozoic—a synthesis. In: Martin, F.J., Chung, S.-L., Lo, C.-H., Lee, T.-Y. (Eds.), Mantle Dynamics and Plate Interactions in East Asia. AGU Geodynamics Series vol. 27, pp. 221–244.

Li, Z.X., Evans, D.A.D., Zhang, S., 2004. A 90° spin on Rodinia: possible causal links between the Neoproterozoic supercontinent, superplume, true polar wander and low-latitude glaciation. Earth Planet. Sci. Lett. 220, 409–421.

Li, Z.X., Zhang, L., Powell, C.McA., 1996. Positions of the East Asian cratons in the Neoproterozoic supercontinent Rodinia. Aust. J. Earth Sci. 43, 593–604.

Lin, J.L., 1984. The Apparent Polar Wander paths for the North and South China Blocks. Ph.D. thesis, University of Calfifornes Santa Barbara, 248 pp.

Lin, J.L., 1988. Middle to Late Proterozoic paleomagnetic results from Jixian. Chinp Sci. Bull. 33, 207–210 (in Chinese).

Lin, J.-L., Fuller, M., Zhang, W., 1985. Preliminary Phanerozoic polar wander paths for the North and South China blocks. Nature 313, 444–449.

Liu, H., 1991. Correlation of Sinian system. In: Liu, H. (Ed.), The Sinian System in China. Science Press, Beijing, pp. 126–170 (Chapter 4, in Chinese).

Lu, S., Li, H., 1991. A precise U–Pb single zircon age determination for the volcanics of Dahongyu Formation, Changcheng System in Jixian. Bull. Chin. Acad. Geol. Sci. 22, 137–146 (in Chinese with English abstract).

McElhinny, M.W., McFadden, P.L., 2000. Paleomagnetism: Continents and Oceans. Academic Press, San Diego, 386 pp.

McFadden, P.L., 1990. A new fold test for paleomagnetic studies. Geophys. J. Int. 103, 163–169.

McFadden, P.L., McElhinny, M.W., 1990. Classification of the reversals test in paleomagnetism. Geophys. J. Int. 103, 725–729.

Meert, J.G., Powell, C.McA., 2001. Assembly and break-up of Rodinia: introduction to the special volume. Precambrian Res. 110, 1–8.

Meng, Q.R., Zhang, G.W., 1999. Timing of the North and South China blocks: controversy and reconciliation. Geology 27, 123–126.

Meng, Q.R., Zhang, G.W., 2000. Geologic framework and tectonic evolution of the Qinling orogen, Central China. Tectonophysics 323, 183–196.

Piper, J.D.A., Zhang, Q.R., 1997. Paleomagnetism of Neoproterozoic glacial rocks of the Huabei shield: the North China Block in Gondwana. Tectonophysics 283, 145–171.

Pisarevsky, S.A., Komissarova, R.A., Khramov, A.N., 2000. New paleomagnetic result from Vendian red sediments in Cisbaikalia and the problem of the relationship of Siberia and Laurentia in the Vendian. Geophys. J. Int. 140, 598–610.

Pisarevsky, S.A., Natapov, L.M., 2003. Siberia and Rodinia. Tectonophysics 375, 221–245.

Pisarevsky, S.A., Wingate, M.T.D., Powell, C.McA., Johnson, S., Evans, D.A.D., 2003. Models of Rodinia assembly and fragmentation. In: Yoshida, M., Windley, B.F., Dasguta, S. (Eds.), Proterozoic East Gondwana Supercontinent Assembly and Breakup. Geological Society (London) Spec. Pub. 206, pp. 35–55.

Powell, C.McA., Li, Z.X., McElhinny, M.W., Meert, J.G., Park, J.K., 1993. Paleomagnetic constrains on timing of the Neoproterozoic breakup of Rodinia and the Cambrian formation of Gondwana. Geology 21, 889–892.

Qiao, X.F., Gao, L., Peng, Y., 2001. Neoproterozoic in Paleo-Tanlu Fault Zone: Catastrophe Sequences Biostratigraphy. Geological Publishing House, Beijing (128 pp., in Chinese).

Qiao, X.F., Gao, M., 1997. Carbonate Pb–Pb isotopic dating of Qingbaikouan system in north China and its significance. Earth Sci. J. Chin. Univ. Geosci. 22, 1–7 (in Chinese with English abstract).

Rainbird, R.H., Stern, R.A., Khudoley, A.K., Kropachev, A.P., Heaman, L.M., Sukhorukov, V.I., 1998. U–Pb geochronology of Riphean sandstone and gabbro from Southeast Siberia and its bearing on the Laurentia–Siberia connection. Earth Planet. Sci. Lett. 164, 409–420.

Reischmann, T., Altenberger, U., Kroener, A., Zhang, G., Sun, Y., Yu, Z., 1990. Mechanism and time of deformation and metamorphism of mylonitic orthogneisses from the Shaogou Shear Zone, Qinling Belt, China. Tectonophysics 185, 91–109.

Smethurst, M.A., Khramov, A.N., Torsvik, T.H., 1998. The Neoproterozoic and Paleozoic paleomagnetic data for the Siberian Platform: from Rodinia to Pangea. Earth Sci. Rev. 43, 1–24.

Sun, D., Li, H., Lin, Y., Zhou, H., Zhao, F., Tang, M., 1991. Precambrian geochronology, Chronotectonic framework and model of chronocrustal structure of the Zhongtiao Mountains. Acta Geol. Sin. 3, 216–231 (in Chinese with English abstract).

Tang, K., 1992. Tectonic Evolution and Minerogentic Regularities of the Fold Belt Along the Northern Margins of Sino-Korean Plate. Peking University Press, Beijing, 277pp. (in Chinese with English abstract).

Torsvik, T.H., Smethurst, M.A., Meert, J.G., Van der Voo, R., McKerrow, W.S., Braiser, M.D., Sturt, B.A., Walderhaug, H.J., 1996. Continental break-up in the Neoproterozoic and Paleozoic—a tale of Baltica and Laurentia. Earth Sci. Rev. 40, 229–258.

Van der Voo, R., 1990. The reliability of paleomagnetic data. Tectonophysics 184, 1–9.

Wang, H., 1986. The Proterozoic. In: Yang, Z., Cheng, Y., Wang, H. (Eds.), The Geology of China. Clarendon Press, Oxford, pp. 48–57.

Wang, H., Li, X., Mei, S., Zhang, S., 1997. Pangaea cycles, Earth's Rhythms and possible earth expansion. In: Wang, H.Z., Jahn, B., Mei, S. (Eds.), Proceedings of the 30th International Geological Congress, vol. 1. International Scientific Publications, Utrecht, pp. 111–128.

Wang, H., Qiao, X., 1984. Proterozoic stratigraphy and tectonic framework of China. Geol. Mag. 121, 599–614.

Wang, H., Zhang S., 2002. Tectonic Pattern of the world Precambrian basement and problems of paleocontinent reconstruction. Earth Sci. J. Chin. Univ. Geosci. 27, 467–481 (in Chinese with English abstract).

Wang, Q., Liu, X., Li, J., 1991. Plate Tectonics Between Cathaysia and Angaraland in China. Peking University Press, Beijing, 151 pp. (in Chinese with English abstract).

Wang, S., Sang, H., Qiu, J., Chen, M., Li, M., 1995. The forming ages of Yangzhuang and Wumishan formations in Jixian section, Northern China. Sci. Geol. Sin. 30, 166–173 (in Chinese with English abstract).

Weil, A.B., Van der Voo, R., Niocaill, C.M., Meert, J.G., 1998. The Proterozoic supercontinent Rodinia: paleomagnetically derived reconstructions for 1100–800 Ma. Earth Planet. Sci. Lett. 154, 13–24.

Xing, Y. (Ed.), 1989. The Upper Precambrian of China. Stratigraphy of China No. 3. Geological Publishing House, Beijing, p. 314 pp (in Chinese).

Yang, Z.Y., Ma, X.H., Huang, B.C., Sun, Z., Zhou, Y., 1998. Apparent polar wander path and tectonic movement of the North China Block in Phanerozoic. Sci. Chin. (D) 41 (Suppl.), 51–65.

Yin, L., Guan, B., 1999. Organic-walled microfossils of the Neoproterozoic Dongjia Formation, Lushan County, Henan Province, North China. Precambrian Res. 94, 121–137.

Zhang, H.M., Zhang, W.Z., 1985. Paleomagnetic data, late Precambrian magnetostratigraphy and tectonic evolution of eastern China. Precambrian Res. 29, 65–75.

Zhang, H.M., Zhang, W.Z., Elston, D.P., 1991. Paleomagnetic study on Middle and Late Proterozoic rock in Jixian, North China. Acta Geophys. Sin. 34, 602–615 (in Chinese with English abstract).

Zhang, S., Li, Z.X., Wu, H., Wang, H., 2000. New paleomagnetic results from the Neoproterozoic successions in southern North China Block and paleogeographic implications. Sci. Chin. (D) 43 (Suppl.), 233–244.

Zhang, W.Z., Li, P., 1980. Paleomagnetism of the Sinian Suberathem in the Jixian, China. Bull. Chin. Acad. Geol. Sci. (Ser. VI) 1, 111–122 (in Chinese with English abstract).

Zhang, Z., Liu, D., Fu, G., 1994. Isotopic Chronology of the Metamorphic Strata from the North Qinling Belt. Geological Publishing House, Beijing, 183 pp. (in Chinese).

Zhao, G., Cawood, P.A., Wilde, S.A., Sun, M., 2002. Review of global 2.1–1.8 Ga orogens: implications for a pre-Rodinia supercontinent. Earth Sci. Rev. 59, 125–162.

Zhao, G., Sun, M., Wilde, S.A., 2003. Correlations between the Eastern Block of the North China Craton and the South Indian Block of the Indian Shield: an Archean to Paleoproterozoic link. Precambrian Res. 122, 201–233.

Zhao, X., Coe, R.S., 1987. Palaeomagnetic constraints on the collision and rotation of North and South China. Nature 327, 141–144.

Zhao, X.X., Coe, R., Liu, C., Zhou, Y., 1992. New Cambrian and Ordovician paleomagnetic poles for the North China Block and their Paleogeographic implications. J. Geophys. Res. 97 (B2), 1767–1788.

Zhao, X.X., Coe, R.S., Gilder, S.A., Frost, G.M., 1996. Palaeomagnetic constraints on the palaeogeography of China: implications for Gondwanaland. Aust. J. Earth Sci. 43, 643–672.

Zhou, H., Wang, Z., Cui, X., Lei, Z., Dong, W., 1996. A study of sequence stratigraphy of Mesoproterozoic and Neoproterozoic in southern north China Platform. J. Chin. Univ. Geosci. 7, 13–19.